

AD-A169 384

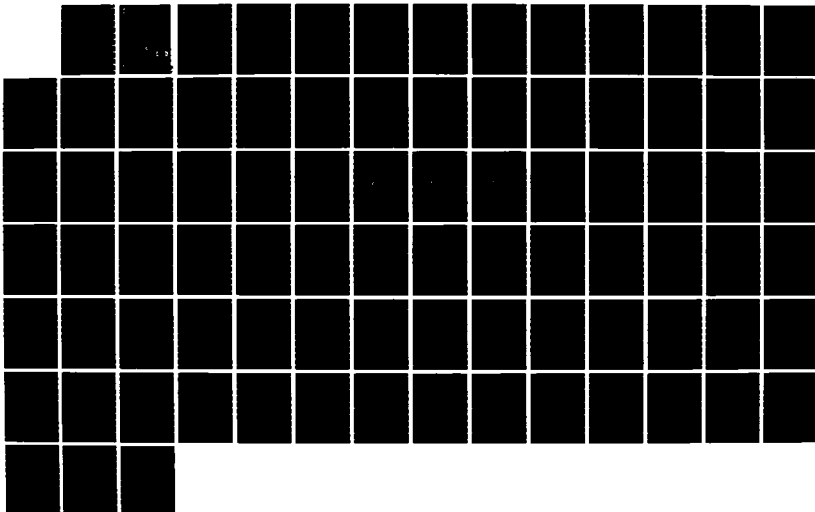
DEVELOPMENT OF A NUMERICAL PROCEDURE TO TREAT WIRES  
ATTACHED TO ARBITRARY. (U) HOUSTON UNIV TX DEPT OF  
ELECTRICAL ENGINEERING D R WILTON ET AL. 15 APR 86  
ARO-21098.1-EL DARG29-83-K-0127

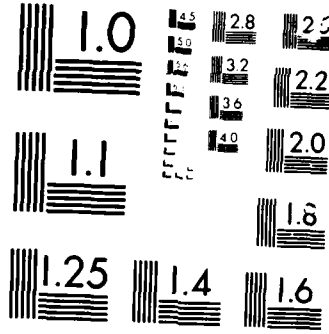
1/1

UNCLASSIFIED

F/G 9/3

NL





MICRONOR

CH 101

AD-A169 384

ARO 21098.1-EL

②

DEVELOPMENT OF A NUMERICAL PROCEDURE  
TO TREAT WIRES ATTACHED TO  
ARBITRARILY SHAPED CONDUCTING BODIES

FINAL REPORT

DONALD R. WILTON  
STUART A. LONG

U.S. ARMY RESEARCH OFFICE  
CONTRACT DAAG-29-83-K-0127



Department of Electrical Engineering

Cullen College of Engineering

University of Houston

This document has been approved  
for public release and sale; its  
distribution is unlimited.

86 7 1 032

DTIC FILE COPY

DEVELOPMENT OF A NUMERICAL PROCEDURE TO TREAT  
WIRES ATTACHED TO ARBITRARILY SHAPED CONDUCTING BODIES

FINAL REPORT

DONALD R. WILTON  
STUART A. LONG

APRIL 15, 1986

U.S. ARMY RESEARCH OFFICE

CONTRACT NUMBER DAAG-29-83-K-0127

UNIVERSITY OF HOUSTON-UNIVERSITY PARK  
DEPARTMENT OF ELECTRICAL ENGINEERING  
HOUSTON, TEXAS 77004

APPROVED FOR PUBLIC RELEASE  
DISTRIBUTION UNLIMITED

UNCLASSIFIED

SECURITY CLASSIFICATION OF THIS PAGE (When Data Entered)

MASTER COPY - FOR REPRODUCTION PURPOSES

REPORT DOCUMENTATION PAGE		READ INSTRUCTIONS BEFORE COMPLETING FORM
1. REPORT NUMBER <i>ARO 21098.1-EL</i>	2. GOVT ACCESSION NO. <i>N/A</i>	3. RECIPIENT'S CATALOG NUMBER <i>N/A ADA 169384</i>
4. TITLE (and Subtitle) Development of a Numerical Procedure to Treat Wires Attached to Arbitrarily Shaped Conducting Bodies		5. TYPE OF REPORT & PERIOD COVERED Final Report September 1, 1983 to February 28, 1986.
7. AUTHOR(s) Donald R. Wilton Stuart A. Long		6. PERFORMING ORG. REPORT NUMBER
9. PERFORMING ORGANIZATION NAME AND ADDRESS University of Houston-University Park Department of Electrical Engineering Houston, Texas 77004		8. CONTRACT OR GRANT NUMBER(s)  DAAG-29-83-K-0127
11. CONTROLLING OFFICE NAME AND ADDRESS U. S. Army Research Office Post Office Box 12211 Research Triangle Park, NC 27709		10. PROGRAM ELEMENT, PROJECT, TASK AREA & WORK UNIT NUMBERS
14. MONITORING AGENCY NAME & ADDRESS (if different from Controlling Office)		12. REPORT DATE April 15, 1986
		13. NUMBER OF PAGES
		15. SECURITY CLASS. (of this report)  Unclassified
		15a. DECLASSIFICATION/DOWNGRADING SCHEDULE
16. DISTRIBUTION STATEMENT (of this Report)  Approved for public release; distribution unlimited.		
17. DISTRIBUTION STATEMENT (of the abstract entered in Block 20, if different from Report)  NA		
18. SUPPLEMENTARY NOTES  The view, opinions, and/or findings contained in this report are those of the author(s) and should not be construed as an official Department of the Army position, policy, or decision, unless so designated by other documentation.		
19. KEY WORDS (Continue on reverse side if necessary and identify by block number)  Wire antennas; finite ground planes; arbitrarily shaped conductors; vehicular antennas.		
20. ABSTRACT (Continue on reverse side if necessary and identify by block number)  A numerical analysis procedure was developed which modeled wire radiating structures, conducting surfaces, and the junctions between them. In addition, an experimental investigation was undertaken to determine the admittance of a monopole antenna attached to a conducting box-a configuration which models several actual radiating systems. Experimental measurements and numerically predicted data were compared with good correlation noted.		

Table of Contents

Statement of Problem.....4

Summary of Important Results.....5

List of Publications.....9

List of Participating Scientific Personnel.....10

Appendix.....11

Accession No.	
FILE	<input checked="" type="checkbox"/>
INDEX	<input type="checkbox"/>
UNCLAS	<input type="checkbox"/>
JUL	
PR	
IN	
	es
	es
Dist	
A-1	



## Statement of Problem

Advanced communications systems are highly dependent on the performance of their antennas. Many of these radiating systems consist of wire elements mounted on ground-based or airborne vehicles. Even fixed antennas may often be erected near the corner or edge of a building roof or near some conducting object whose presence affects the radiating characteristics of the antenna. Such systems, consisting of wire elements that have a ground plane that cannot be treated as essentially planar and infinite in extent are not easily analyzed or designed. Frequently the design process is interrupted by changes in the mounting platform, in the antenna configuration, or in the operating environment of the antenna.

To aid in these problems, a two-fold investigation of the problem of a wire antenna mounted on an arbitrarily shaped conducting body has been undertaken. First, a numerical analysis procedure has been developed which models the wire structures, the conducting surfaces, and the junctions between them. Second, careful experimental measurements have been made for specific cases of monopole antennas attached to conducting bodies that model important practical applications.

## Summary of Important Results

### A. Analytical and Numerical Work

The primary thrust of the analytical and numerical portion of this research is the modeling of currents in the neighborhood of wire-to-body junctions. For this purpose, special basis functions for use in the solution of integral equations involving unknown surface and wire currents have been developed. We have shown from a quasistatic analysis that the radial component of surface current varies as  $1/r$  in the neighborhood of the wire attachment point irrespective of the surface geometry at the point. For enhanced accuracy, this  $1/r$  variation has been incorporated into the basis functions representing surface current in the vicinity of the attachment point.

Numerical solution of integral equations for wire and surface induced currents by the method of moments requires the computation of both vector scalar potentials associated with the currents. The junction basis functions have been carefully constructed so that their associated charge distributions and, therefore, their scalar potential contributions, are identical to those of the basis functions representing the ordinary surface currents. The computation of vector potential contributions, on the other hand, required the development of new numerical and analytical methods. This involved a major part of the effort since these integrals are complicated by the fact that the basis functions are vector-valued, are defined over triangular patches representing the surface, and have  $1/r$  singularities at the attachment points (assumed to be at triangle vertices). The vector potential integrals also contain a second singularity whenever the point at which the potential is being observed falls within the source triangle. A rather involved combination of analytical and numerical techniques has been developed to efficiently handle the evaluation of such integrals.

As mentioned above, the radial variation of the radial component of the current near the wire attachment point is known to be  $1/r$ ; the angular variation, however, depends on the surface geometry at the attachment point. Two different approaches were considered for modeling this behavior:

1. The region around the attachment point may be subdivided into small angular regions and independent junction basis functions may be defined for each region. The angular distribution would then be numerically determined during the course of the solution process. The approach is attractive in that no a priori assumptions on the current distribution need be made. However, it has the



dual disadvantages that a large number of unknowns must be introduced to model a junction and that the basis functions are nearly linearly dependent with respect to the ordinary surface basis functions near the wire attachment point. The latter difficulty may be removed by appropriately discarding or constraining certain basis functions, but a very involved programming logic is required. For these reasons, this approach was not selected.

2. The angular distribution of the current about the attachment point is essentially that of the magnetostatic current distribution on a equivalent "tangent" geometry at the point. The tangent geometry consists of a conical surface whose generators are tangent to the actual surface at the attachment point together with a linear filament of current tangent to the wire axis at the attachment point. The magnetostatic current distribution on this tangent geometry for a unit filament current may be easily computed via numerical solution of a simple integral equation, and the result may be used to appropriately distribute the current in the basis functions surrounding the attachment point. The total axial current entering the wire is then the only unknown junction quantity that must be numerically determined. A minor inconvenience of this approach is that an auxiliary problem must be solved. It is possible, however, to incorporate the solution of the auxiliary problem as a part of setting up the problem geometry so that it is independent of the solution step.

In parallel with the effort to develop a numerical technique for modeling wires attached to surfaces, a significant effort was also made during the project to enhance the capabilities of the triangular patch surface modeling code. Except as noted below, implementation of these improvements has been a joint effort with Dr. William A. Johnson and others at Sandia National Laboratories. Among the advanced features and enhancements added to the surface patch and wire modeling codes were the following:

Personnel at Sandia essentially rewrote the surface patch code in a structured programming format in order to improve its readability and maintainability.

The code was upgraded to permit the treatment of multiple conducting bodies and intersecting surfaces.

The large memory capacity of current mainframe computers made it feasible to consider storing a number of frequently used quantities to improve efficiency. This modification and the inclusion of an adaptive integration algorithm considerably improved the efficiency of the program.

A new program for treating an arbitrary configuration of wires was developed. Among important features of the new approach are improved efficiency, better treatment of mutual coupling between closely spaced wires, and a programming structure that closely parallels that of the triangular patch code. The two codes were then merged into a single general-purpose code for treating arbitrary configurations of conducting bodies and wires.

The capability to treat voltage sources and/or lumped loads placed across body edges or wire segments was introduced into all the code.

The capability to exploit any symmetry present in a scattering or radiation problem was implemented at Sandia. The presence of symmetry in a given problem can significantly reduce the computer resources necessary to solve the problem. The present version of these codes permits up to three mutually perpendicular symmetry planes of either electric or magnetic type. This capability was found to be essential in allowing us to compare calculated and experimental results.

The group at Sandia also developed a capability to compute near fields. The specializations of that feature required to permit the efficient computation of far fields was implemented at the University of Houston.

A very useful interactive geometry generation program was developed at Sandia. The program permits an arbitrary conducting body to be built up out of a number of canonical shapes such as cylinders, spheres, cones, etc. This new feature, combined with a graphical representation of surface patch models, is extremely helpful in setting up geometries for numerical solution.

It is anticipated that a version of the code combining all these features and an accompanying user's guide will be made available.

## B. Experimental Work

In an attempt to provide accurate verification of the analytical results, as well as data for very specific practical cases, the experimental work concentrated on an investigation of a monopole attached to a conducting box. Special attention was given to the behavior of the input admittance of the monopole both as a function of the electrical size of the box and the position of the monopole with respect to an edge or corner. This configuration closely models the very practical cases of antennas mounted on buildings or vehicles.

To facilitate the measurements, a cubical conducting box was fabricated and mounted on a ground plane. Various length monopoles were then mounted on top of the box at positions along a line from the center of the box to the center of one edge. In a similar fashion the same monopoles were then moved along a diagonal line from the center to one corner of the top of the box. Input admittance data were carefully taken as a function of frequency near the resonance of the monopole. From this data variations in resonant frequency, peak conductance, and quality factor were then calculated and their dependence on feed position and box size deduced.

The details of the experimental apparatus and procedures along with the actual data that was obtained is included in the appendix of this report. The key results are tabulated and graphed and empirical insight into the problem is provided.

In addition, numerically calculated values of admittance are compared with the experimental data. The correlation was remarkably high for cases for which the patch size remained small compared to the wavelength. The details of these comparisons are also shown in the appendix.

The experimental portion of the work accomplished two major tasks. The first was its verification of the ability of the numerical analysis techniques to accurately model the radiating structure. Secondly, and perhaps equally important, the data generated allows the general behavior of the antenna characteristics to be predicted empirically as the monopole approaches an edge or corner of a conducting body.

### List of Publications

"Potential Integrals for Uniform and Linear Source Distributions on Polygonal and Polyhedral Domains" D. R. Wilton, S. M. Rao, A. W. Glisson, D. H. Schaubert, O. M. Al-Bundak, and C. M. Butler, IEEE Trans. Antennas and Propagation, Vol. AP-32, No. 3, March 1984, pp. 276-281.

"Current Progress in the Development of and Modeling with the Electric Field Integral Equation Surface Patch Code," W. A. Johnson, K. M. Damrau, D. R. Wilton, R. M. Sharpe, and S. U. Hwu, 1985 IEEE Antennas and Propagation Society International Symposium Digest, Vancouver, Canada, June 1985, p. 263.

"An Investigation of a Monopole Antenna Attached to a Conducting Box," S. Bhattacharya, S. A. Long, and D. R. Wilton, National Radio Science Meeting Digest, Boulder, Colorado, January 1986, p. 229.

"A Numerical Approach to Modeling Wires Attached to Surfaces," D. R. Wilton and S. U. Hwu, 1986, National Radio Science Meeting Digest, Philadelphia, PA, June 1986.

"The Admittance of a Monopole Antenna Attached to a Conducting Box," S. Bhattacharya, S. A. Long, and D. R. Wilton, in preparation for the IEEE Transactions on Antennas and Propagation.

"Numerical Modeling of Wires Attached to Conducting Surfaces," S. U. Hwu and D. R. Wilton, in preparation for the IEEE Transactions on Antennas and Propagation.

"Computation of Quasi-Static Current Distributions Near Wire-To-Surface Junctions," Q. Chen and D. R. Wilton, in preparation for the IEEE Transactions on Antennas and Propagation.

List of Participating Scientific Personnel

Donald R. Wilton - Professor

Stuart A. Long - Professor

Surendra Singh - Ph.D., August 1985, "Numerical Modeling of  
Infinite Phased Arrays of Wire and Slot Elements

Shyamal Bhattacharya - M.S., April 1986, "A Study of the  
Admittance Characteristics of a Monopole  
Antenna Attached to a Conducting Box

Robert Sharpe - Graduate Research Assistant

Shian-Uei Hwu - Graduate Research Assistant

Quinglum Chen - Graduate Research Assistant

# Appendix

# Contents

<b>A Introduction</b>	<b>1</b>
<b>B Experimental Procedure</b>	<b>4</b>
<b>C Experimental Results</b>	<b>10</b>
<b>D Numerical Analysis</b>	<b>43</b>
<b>E Conclusion</b>	<b>66</b>

# List of Figures

B.1	Geometry of the box over ground plane . . . . .	7
B.2	Name of monopole feed positions . . . . .	8
B.3	Block diagram for automated data collection system . . . . .	9
C.1	6 cm monopole on box over ground plane; feed position varies along the diagonal . . . . .	15
C.2	6 cm monopole on box over ground plane; feed position varies along the center-line . . . . .	16
C.3	5 cm monopole on box over ground plane; feed position varies along the diagonal . . . . .	17
C.4	5 cm monopole on box over ground plane; feed position varies along the center-line . . . . .	18
C.5	4 cm monopole on box over ground plane; feed position varies along the diagonal . . . . .	19
C.6	4 cm monopole on box over ground plane; feed position varies along the center-line . . . . .	20
C.7	3 cm monopole on box over ground plane; feed position varies along the diagonal . . . . .	21
C.8	3 cm monopole on box over ground plane; feed position varies along	



the center-line . . . . .	22
C.9 2 cm monopole on box over ground plane; feed position varies along the diagonal . . . . .	23
C.10 2 cm monopole on box over ground plane; feed position varies along the center-line . . . . .	24
C.11 Quality factor versus distance from center; 6 cm monopole . . . . .	25
C.12 Quality factor versus distance from center; 5 cm monopole . . . . .	26
C.13 Quality factor versus distance from center; 4 cm monopole . . . . .	27
C.14 Quality factor versus distance from center; 3 cm monopole . . . . .	28
C.15 Quality factor versus distance from center; 2 cm monopole . . . . .	29
C.16 Peak conductance versus distance from center; 6 cm monopole . . . .	30
C.17 Peak conductance versus distance from center; 5 cm monopole . . . .	31
C.18 Peak conductance versus distance from center; 4 cm monopole . . . .	32
C.19 Peak conductance versus distance from center; 3 cm monopole . . . .	33
C.20 Peak conductance versus distance from center; 2 cm monopole . . . .	34
C.21 Zero crossing frequency versus distance from center; 6 cm monopole .	35
C.22 Zero crossing frequency versus distance from center; 5 cm monopole .	36
C.23 Zero crossing frequency versus distance from center; 4 cm monopole .	37
C.24 Zero crossing frequency versus distance from center; 3 cm monopole .	38
C.25 Zero crossing frequency versus distance from center; 2 cm monopole .	39
C.26 Peak conductance versus monopole length . . . . .	40
C.27 Zero crossing frequency versus monopole length . . . . .	41
C.28 Quality factor versus monopole length . . . . .	42
D.1 Patch model; monopole at box center; front view . . . . .	48
D.2 Patch model; monopole at box edge; front view . . . . .	49
D.3 Patch model; monopole at box corner; front view . . . . .	50

D.4	6 cm Monopole at box center . . . . .	51
D.5	6 cm Monopole at box edge(center-4) . . . . .	52
D.6	6 cm Monopole at box corner(diagonal center-5) . . . . .	53
D.7	5 cm Monopole at box center . . . . .	54
D.8	5 cm Monopole at box edge(center-4) . . . . .	55
D.9	5 cm Monopole at box corner(diagonal center-5) . . . . .	56
D.10	4 cm Monopole at box center . . . . .	57
D.11	4 cm Monopole at box edge(center-4) . . . . .	58
D.12	4 cm Monopole at box corner(diagonal center-5) . . . . .	59
D.13	3 cm Monopole at box center . . . . .	60
D.14	3 cm Monopole at box edge(center-4) . . . . .	61
D.15	3 cm Monopole at box corner(diagonal center-5) . . . . .	62
D.16	2 cm Monopole at box center . . . . .	63
D.17	2 cm Monopole at box edge(center-4) . . . . .	64
D.18	2 cm Monopole at box corner(diagonal center-5) . . . . .	65

## Appendix A

### Introduction

The monopole antenna mounted on an infinite ground plane has received much attention in the past, and recently monopole antennas mounted on arbitrary shaped objects have been investigated. This thesis primarily concerns a monopole antenna mounted on a cubical box over a ground plane. By varying the location of the antenna on the 'box', the effect on the circuit parameters such as input impedance, peak admittance, quality factor, resonant frequency and zero crossing of input susceptance can be investigated.

In practice, however, antennas are mounted on quite arbitrarily shaped objects such as aircraft, vehicles, ships, buildings, etc. Even in the case of arbitrarily shaped objects, the antennas are not always centrally mounted. The objective of this investigation is to determine how the circuit parameters are affected as the position of the antenna on the object changes, especially near edges and corners and as the electrical size of the box changes. Monopole lengths of 6 cm, 5 cm, 4 cm, 3 cm and 2 cm are considered in the investigation.

M. Marin and M. F. Catedra [1] have discussed the evaluation of input impedance of a monopole located at any point on a circular disc oriented in an arbitrary direction using the moment method and geometrical theory of diffraction techniques.

The agreement between the numerical analysis and experimental results has been shown to be excellent in that paper.

D. M. Pozar and E. H. Newman [2] have investigated monopoles mounted near an edge or a vertex of an object. Several others have calculated the input impedance of a monopole antenna at the center of a finite size ground plane. In this thesis a comparison of the input admittance of a monopole antenna at the box center over a ground plane is made with that of a monopole at the center of a finite ground plane.

K. H. Awadalla and T. S. M. Maclean [3] have investigated the input impedance of a monopole antenna over a finite size, square conducting plane. The oscillatory behavior of the input impedance for a quarter wavelength monopole at the center of a square disc of finite length has been shown in the above mentioned article.

A cubical conducting box over a ground plane was fabricated in such a way as to facilitate mounting the antenna at different locations on the box. The position of the antenna could be shifted along a line from the center of the box out to the center of an edge. Also there were provisions to move the position of the antenna from the center of the box to the corner of the box along a diagonal line.

Admittance plots were obtained using a Hewlett Packard Model 8410B network analyzer for several different positions of the antenna. From these plots peak admittance, quality factor and other circuit parameters of interest were computed.

In this thesis an attempt has been made to compare experimental results of input admittance with that obtained by numerical analysis utilizing a method of moment technique with triangular patches. A mathematical model of the conducting box was constructed using triangular patches. S. M. Rao, D. R. Wilton and A. W. Glisson [4] previously developed a numerical technique to solve electromagnetic scattering problems by surfaces of arbitrary shape using the method of moments.

A modified version of this technique contained in the computer code PATCH is used in the numerical analysis to compute the input admittance of a monopole on a conducting box.

The impedance matrix was formulated using the electric field integral equation with an appropriate boundary condition and the unknown currents through the triangular patch edges were found for a unit voltage source applied at the junction of the base of the monopole and the top surface of the box. Experimental results of input admittance were compared with the computed results for several different positions of the antenna on the box.

## Appendix B

# Experimental Procedure

The purpose of this experiment was to determine and study circuit parameters such as input admittance, zero crossing frequency of the input susceptance and peak input conductance of a monopole antenna mounted on a cubical conducting box over a ground plane as shown in Figure B.1. It was also important to find the effects on these circuit parameters due to the changes in the position of the antenna on the cubical box, because in practice the antennas are not always centrally mounted on an object. One other aspect of this investigation was to determine how a monopole on the box center over a ground plane compares with a monopole at the center of a finite size ground plane.

The geometry and dimensions of the cubical box are shown in Figure B.1 and Figure B.2. The box is a 10 cm cube and the ground plane size is 78.0 cm x 78.0 cm. The bottom face of the cubical box is open so that a 50 ohm coaxial cable can be connected to the antenna probe. There were several pre-drilled holes on the top surface of the box to facilitate installation of the monopole antenna at different positions on the box. Figure B.1 shows the distances of those holes with respect to the center of the box. There are two rows of holes on the box top, one to vary the position of the antenna along a line joining the center of the box to the center

of an edge and the other to vary the position along a diagonal. Each hole has been given a name relative to its position from the center (Figure B.2). The hole at the center of the box is quite appropriately called "center". Holes along a line joining the center to the center of an edge are called 'center-1', 'center-2', 'center-3' and 'center-4', starting with 'center-1' nearest to the center of the box. The holes along the diagonal are called 'diagonal center-1', ..., 'diagonal center-5' inclusive, with 'diagonal center-1' being nearest to the center of the box. Distances of all the holes (feed-positions) from the center of the box are shown in Figure B.1.

The antennas installed on the box over the ground plane were tested using a Hewlett Packard Network Analyzer. The block diagram for the system configuration is shown in Figure B.3. The following is a list of equipment used for the measurements.

*HP 9816 Personal Computer*

*HP 9121 Disc Drive*

*HP 7470A 2-Pen Graphics Plotter HP 82905B Printer*

*HP 8620C Sweep Oscillator with HP 8624A RF Plug-In*

*EIP 545A Microwave Frequency Counter*

*HP 8743A Reflection/Transmission Test Unit*

*HP 59313A HP IB Analog to Digital Converter*

*HP 8410B Network Analyzer with HP 8414A Polar Display*

*HP 8411A Harmonic Frequency Converter*

*HP 779D Coaxial Directional Coupler*

The monopole antennas were made of brass rod 1.6 mm in diameter. The lengths were fabricated such that the rod projected 6 cm, 5 cm, 4 cm, 3 cm and 2 cm above the top surface of the box. One end of the brass rod was connected to an SMA coaxial connector (Amphenol Model No. 901-9215). The flange of the connector

was connected to the under side of the top plate of the cubical box with four screws. The monopole antennas were connected to a Hewlett Packard Reflection Test Set (Model No. HP 8743A) by the coaxial feed cable.

The procedure for taking measurements consisted of selecting a range of frequency to include the first resonance of the monopole, calibrating the Reflection Test Set with a short circuit load at the end of a 12 cm long, 50 ohm coaxial cable and then taking measured values of reflection coefficient at specified intervals sweeping over the frequency range. This process was fully automated using a Hewlett Packard 9816 computer. The software for this automated measurement capability was written by Dr. William F. Richards of the University of Houston. Some of this software was then modified by the author of this thesis. The impedance and admittance values were computed from the measured values of the reflection coefficient and were stored on diskettes for future use or for plotting admittance versus frequency and Smith chart plots.

A 60 cm x 60 cm ground plane was constructed to take admittance measurements of approximately the same lengths of monopoles at the center of this ground plane. This was done to compare admittance values of monopoles over the ground plane with that of a monopole at the center of the box over a ground plane.

The explanation of the captions for admittance versus frequency plots is as follows. The position of the monopole antenna on the box top along a line from the center of the box to the center of an edge is denoted as center-1, center-2 etc. Therefore "6 cm monopole on box center-1" indicates that the monopole is 6 cm long and it is located at the feed next to the center along a line from the center to the center of an edge. Similarly the position of the antenna could be varied along a diagonal line from the center of the box to the corner and plots of those cases are captioned as "diagonal center-1", "diagonal center-2" etc.



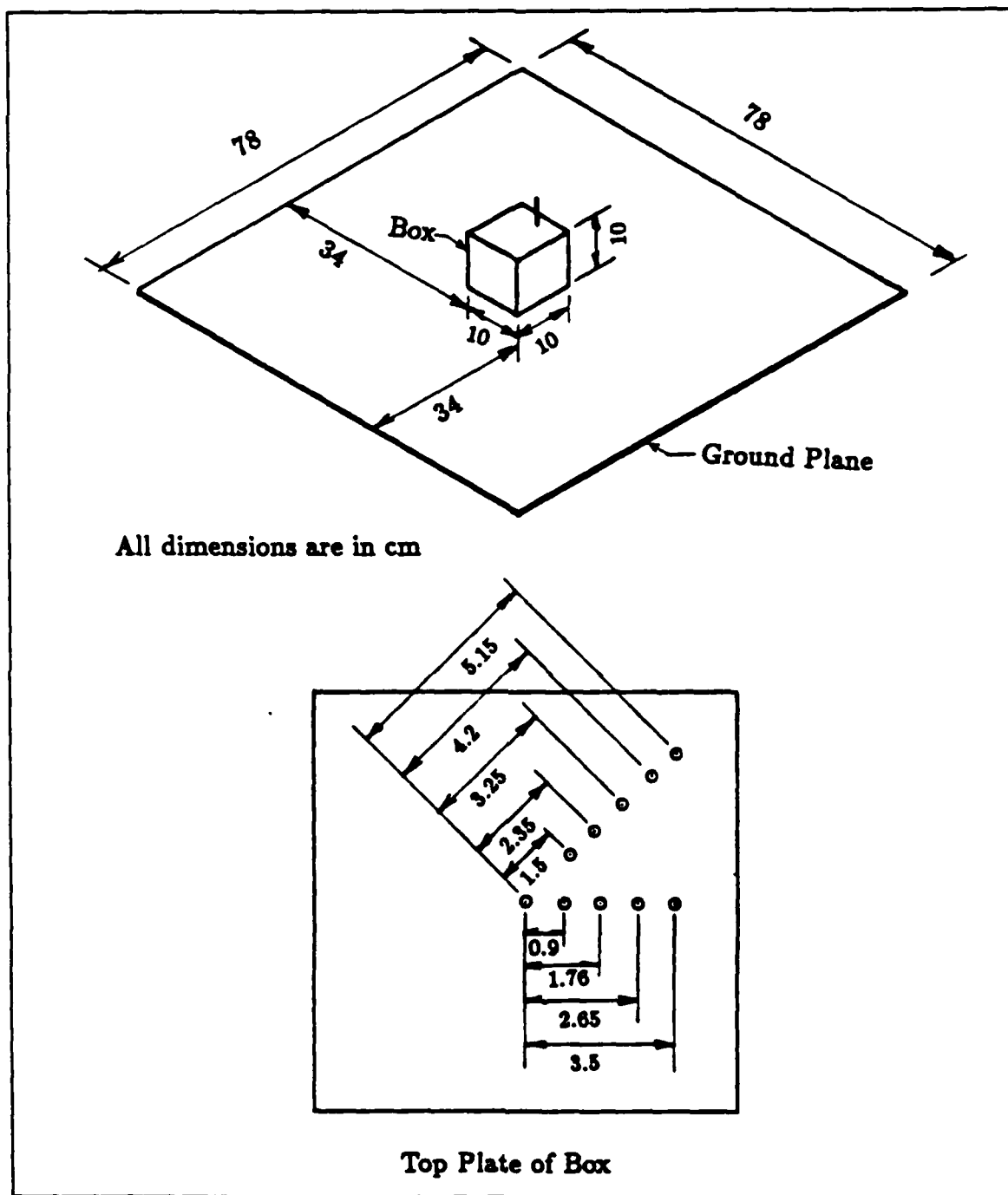


Figure B.1: Geometry of the box over ground plane

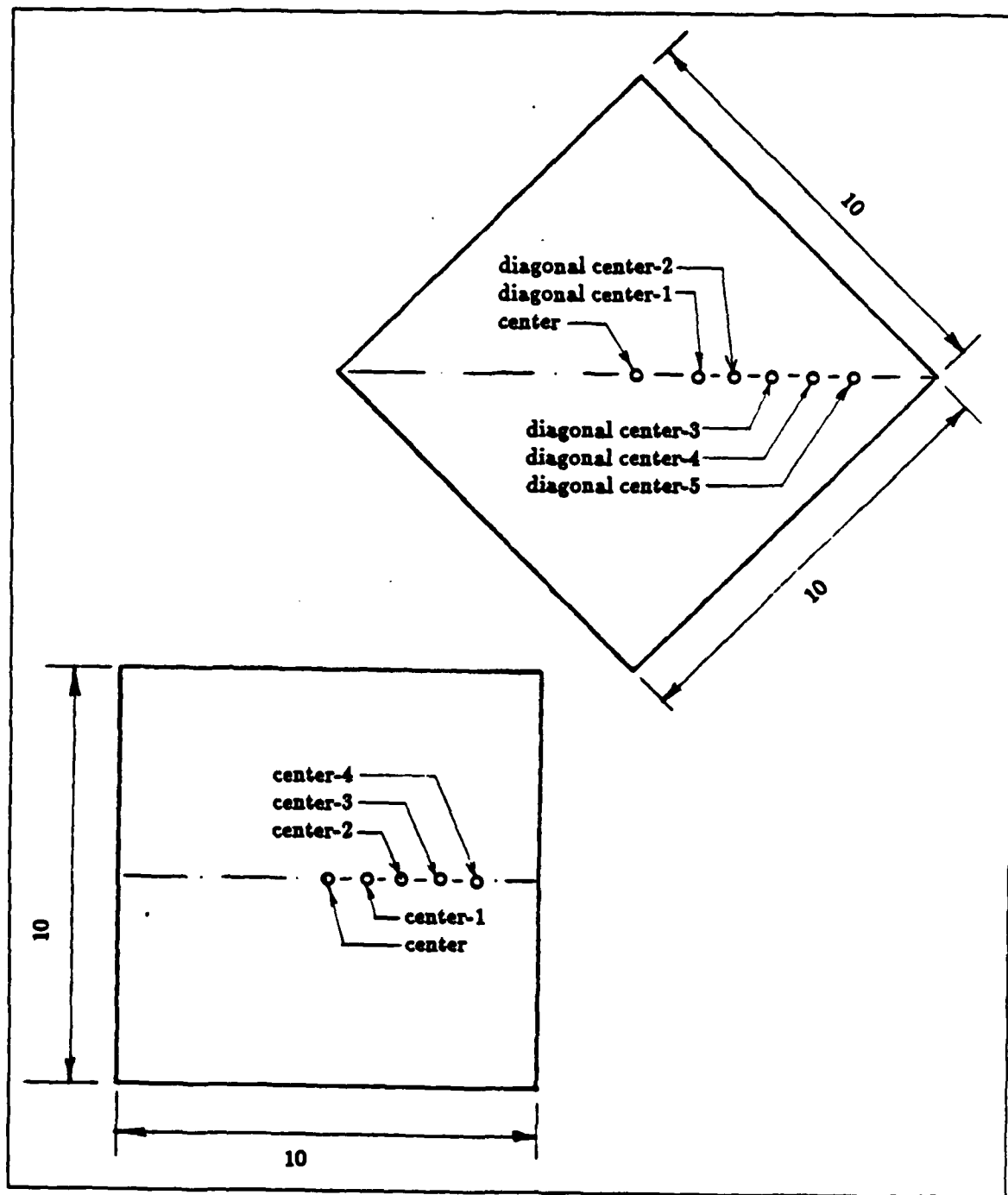


Figure B.2: Name of monopole feed positions

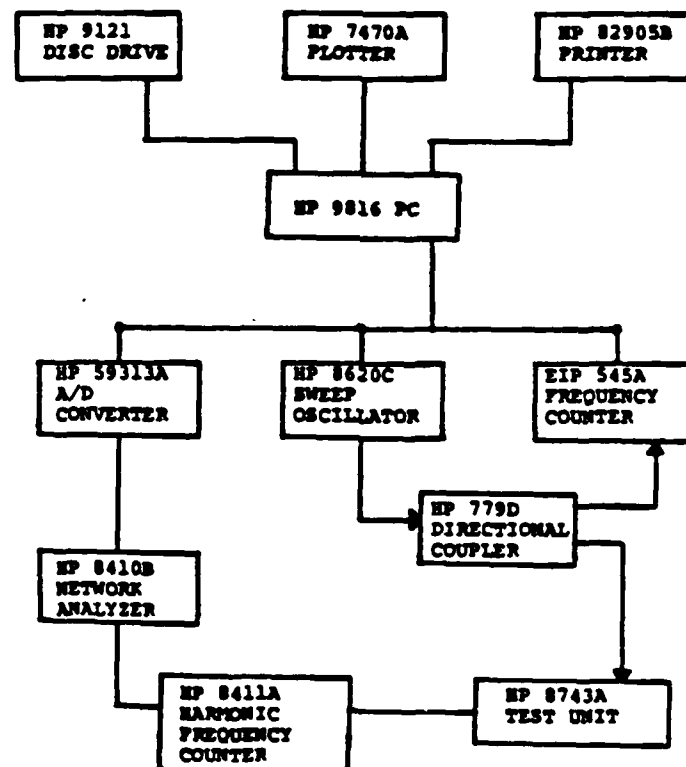


Figure B.3: Block diagram for automated data collection system

## Appendix C

# Experimental Results

The position of the monopole antenna could be varied along a line from the center of the box to an edge or from the center of the box to a corner along a diagonal. This allowed us to determine how the impedance or admittance varied as the position of the monopole antenna was changed. Also monopoles of different lengths were tested to investigate the functional dependence of the input admittance on the electrical size of the box.

Plots of admittance versus frequency for monopoles on a box over a ground plane are presented in Figures C.1 through C.10. Figures C.1 through C.10 show input admittance plots for 6 cm, 5 cm, 4 cm, 3 cm and 2 cm monopoles on the box over a ground plane as the monopole feed position moves along a line from the center of the box to the center of an edge or the corner of the box. For each length of the monopole, two plots of admittance versus frequency are included; one shows superimposed admittance versus frequency plot as the monopole moves along the centerline toward the edge and the other for the monopole position moving along the diagonal toward the corner of the box. For the 6 cm monopole case (Figure C.2), the zero crossing frequency of the input susceptance increases from 1.138 GHz to 1.164 GHz as the monopole position moves from the center to an edge.

This is approximately an increase of 2.3 percent in the zero crossing frequency of the input susceptance. But as the monopole feed position moves from the center to the corner along a diagonal (Figure C.1), the zero crossing frequency of the input susceptance changes from 1.138 GHz to 1.192 GHz which is a 4.7 percent increase. The admittance plots for the other lengths of monopoles exhibit similar qualitative behavior and they are shown in Figures C.3 through C.10.

The peak of the real part of the input admittance, which is shown by the solid line in Figures C.1 through C.10, decreases as the feed position of the monopole moves away from the center. When the feed position of the 6 cm monopole (Figure C.2) moves from the center to the center of an edge, the peak conductance changes from 46.4 m-mhos to 31.7 m-mhos; a 31.7 percent decrease. But, as the feed position moves along a diagonal (Figure C.1) from the center to the corner of the box, the peak of the real part of the input admittance varies from 46.4 m-mhos to 20.9 m-mhos. This is a 55 percent decrease. Figures C.3 thru C.10 show the admittance plots for 5 cm, 4 cm, 3 cm and 2 cm long monopoles. These plots also show a decrease in peak conductance as the monopole feed position moves from the center to the edge or the corner of the box. The admittance plot for a 2 cm long monopole is shown in Figures C.9 and C.10 which shows that the peak conductance increases slightly before it drops as the monopole moves away from the center to either the edge or the corner of the box. The resonant frequency for a 2 cm monopole is large and the box edges are electrically larger. Therefore constructive and destructive interference probably causes this minor deviation to happen.

It is observed from the previously mentioned figures that the frequency at which a peak in the real part of the admittance occurs is different from the zero crossing frequency of the input susceptance. For this reason, the quality factor  $Q_c$  is defined to be the ratio of the frequency at which the magnitude of the admittance peaks to

the fractional bandwidth between the 0.707 of peak magnitude points. The quality factor for different lengths of monopoles and for different positions of the monopole are computed from the measured data. The effects of position of the monopole on the quality factor, the zero crossing frequency of the input susceptance and the peak conductance are shown in Figures C.11 through C.26 for 6 cm, 5 cm, 4 cm, 3 cm and 2 cm monopoles. The quality factor is plotted against distance of the monopole feed from the center of the box.

It is observed that the quality factor gradually decreases as the feed position of the monopole moves away from the center. When the feed position of the 6 cm monopole moves from the center of the box to the corner of the box along a diagonal line (Figure C.11), the quality factor changes from 4.74 to 2.17, which is a 54.3 percent decrease. The quality factor decreases from 4.74 to 3.27, which is only a 31 percent decrease, when the feed position of the 6 cm monopole moves from the center to the center of an edge. Plots of quality factor versus distance of feed position from the center of the box for other lengths of monopoles are shown in Figures C.12 through C.15. For 5 cm, 4 cm, 3 cm and 2 cm monopoles, the quality factor plots show some occasional deviations from the monotonically decreasing behavior.

The effect of position of the monopole on the peak value of the input conductance is clearly shown in Figures C.16 through C.20 for different lengths of monopoles. The peak conductance is plotted against the distance of the monopole from the center of the box. The peak conductance is maximum when the monopole is at the center of the box and gradually decreases as the monopole position shifts towards the edge or the corner of the box. Again for the 2 cm monopole, the peak conductance actually increases slightly before it sharply falls off as the monopole position shifts towards the edge or the corner of the box.

The zero crossing frequencies versus distance of the monopole from the center of the box are presented in Figures C.21 through C.25 for different lengths of monopoles. These plots show that the zero crossing frequency of the input susceptance increases monotonically as the monopole feed moves away from the center toward the edge or the corner of the box. For the 2 cm monopole, there is a slight deviation from the monotonically increasing behavior which may be due to experimental error.

Figure C.26 shows a plot of peak conductance versus monopole length for two separate cases. The 'stars' indicate how the peak conductance varies with different lengths of monopoles at the box center and the 'triangles' are for a monopole at the center of a finite size ground plane. Both plots show an oscillatory type of behavior.

The zero crossing of input susceptance versus monopole length is shown in Figure C.27 for monopoles at the box center and monopoles at the center of a finite size ground plane. The two curves almost overlap each other and both are monotonically decreasing in frequency as the length of the monopole increases. It appears that the monopole at the box center behaves qualitatively in much the same way as the monopole at the center of a finite sized ground plane.

The comparison of quality factor for the two cases mentioned above, however, is not so straight-forward because the quality factor is a function of both the length of the monopole and the diameter of the the monopole. In this investigation the diameter of the antenna did not change. R. W. P. King [5] presented a table listing the theoretical quality factor of monopole antennas for various  $h/a$  ratios where  $h$  is the length of monopole and  $a$  is the radius of the monopole. The actual values of quality factor for the  $h/a$  ratios used in the experiment had to be interpolated from that table. Figure C.28 shows a plot of quality factor against length of monopole for three different cases. Stars represent computed values of quality factor for the

monopole at the box center. Computed values of quality factor for monopoles on a finite ground plane are represented by hexagons and triangles indicate interpolated values of theoretical quality factor . The quality factor for a monopole at the box center shows peaks at discrete frequencies whereas the measured quality factors for the monopole over a finite size ground plane and the theoretical quality factors for the monopole over an infinite ground plane are monotonically increasing functions.



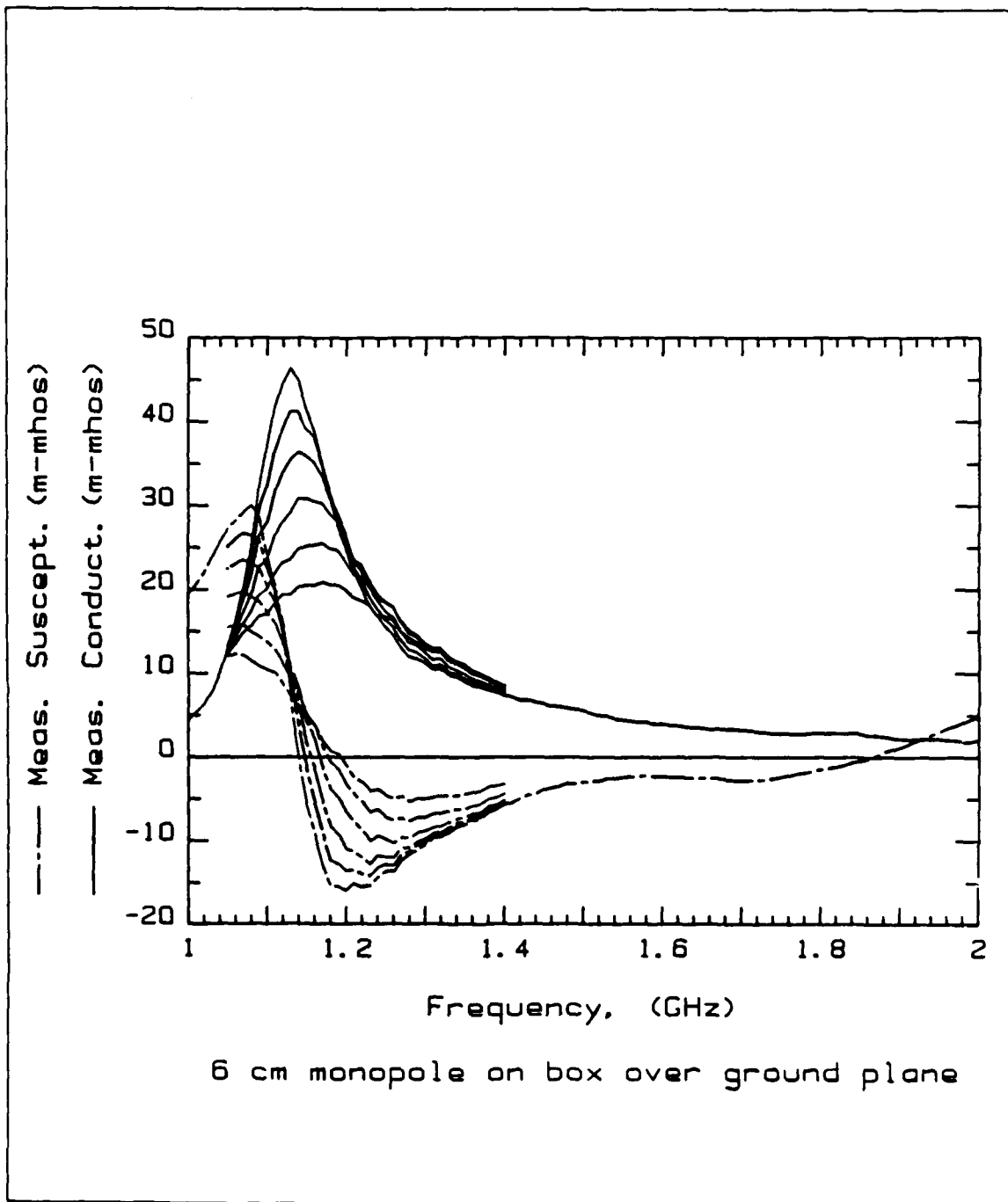
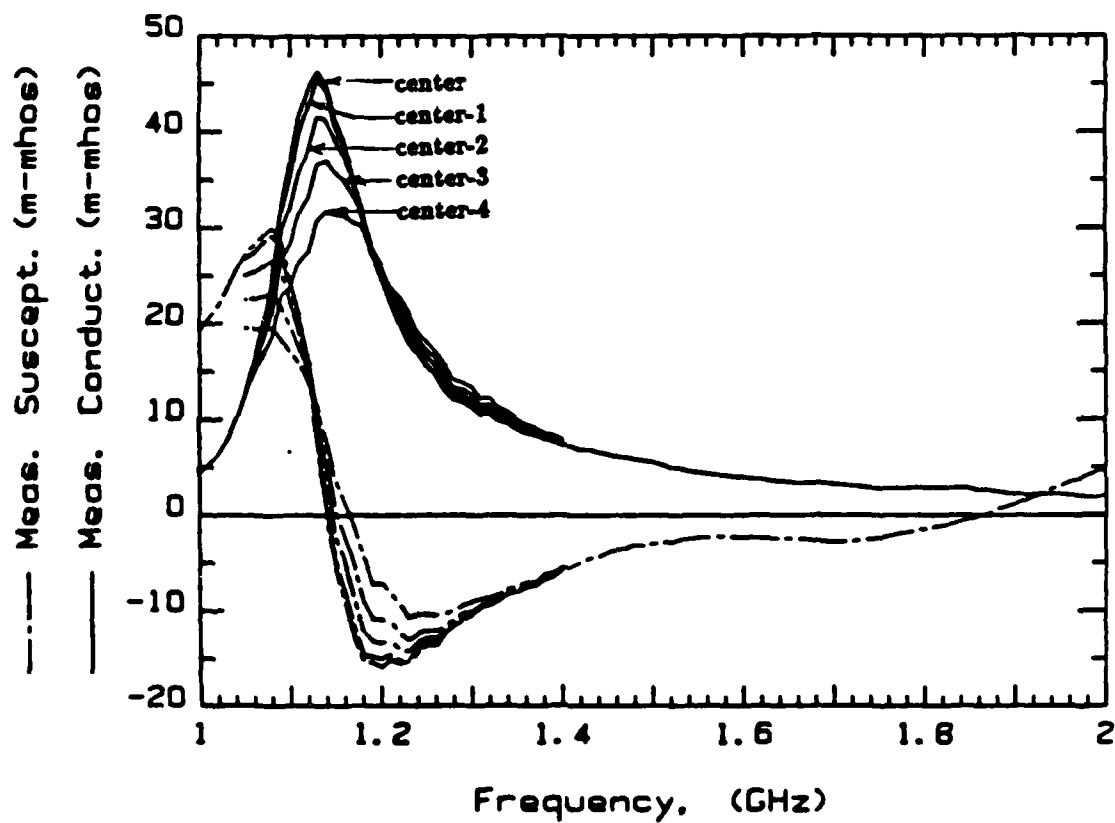


Figure C.1: 6 cm monopole on box over ground plane; feed position varies along the diagonal



6 cm monopole on box over ground plane

Figure C.2: 6 cm monopole on box over ground plane; feed position varies along the center-line

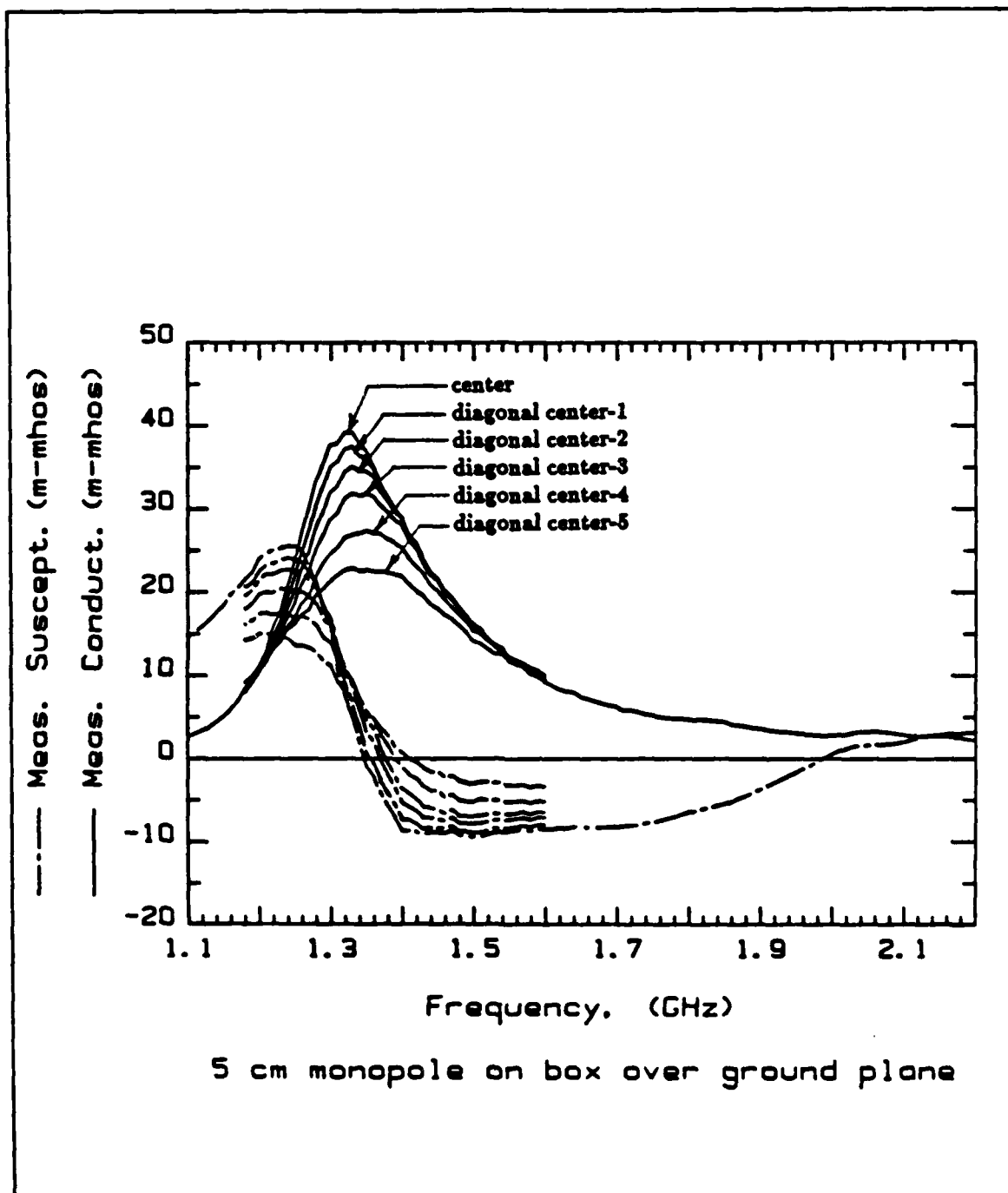


Figure C.3: 5 cm monopole on box over ground plane; feed position varies along the diagonal

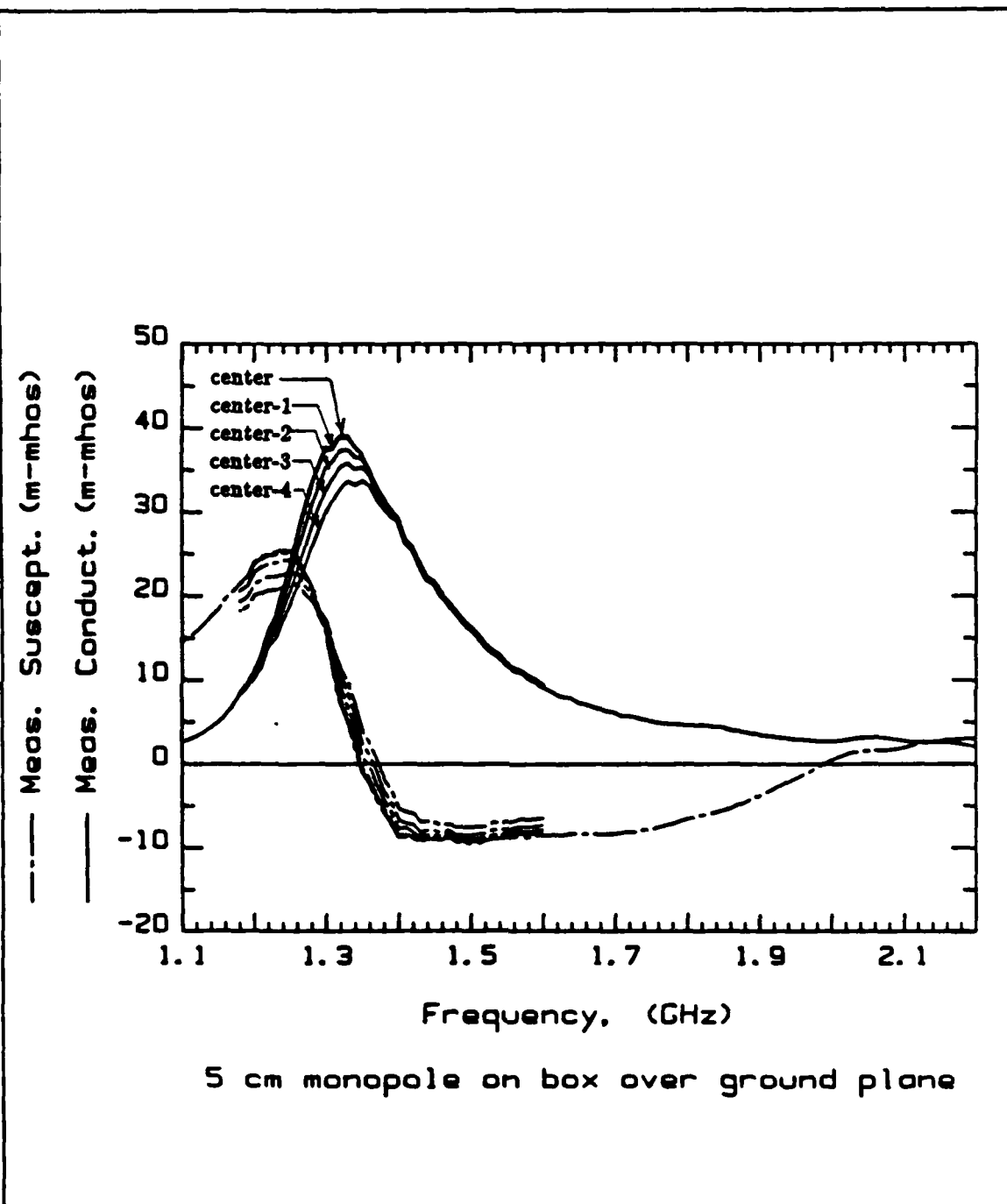
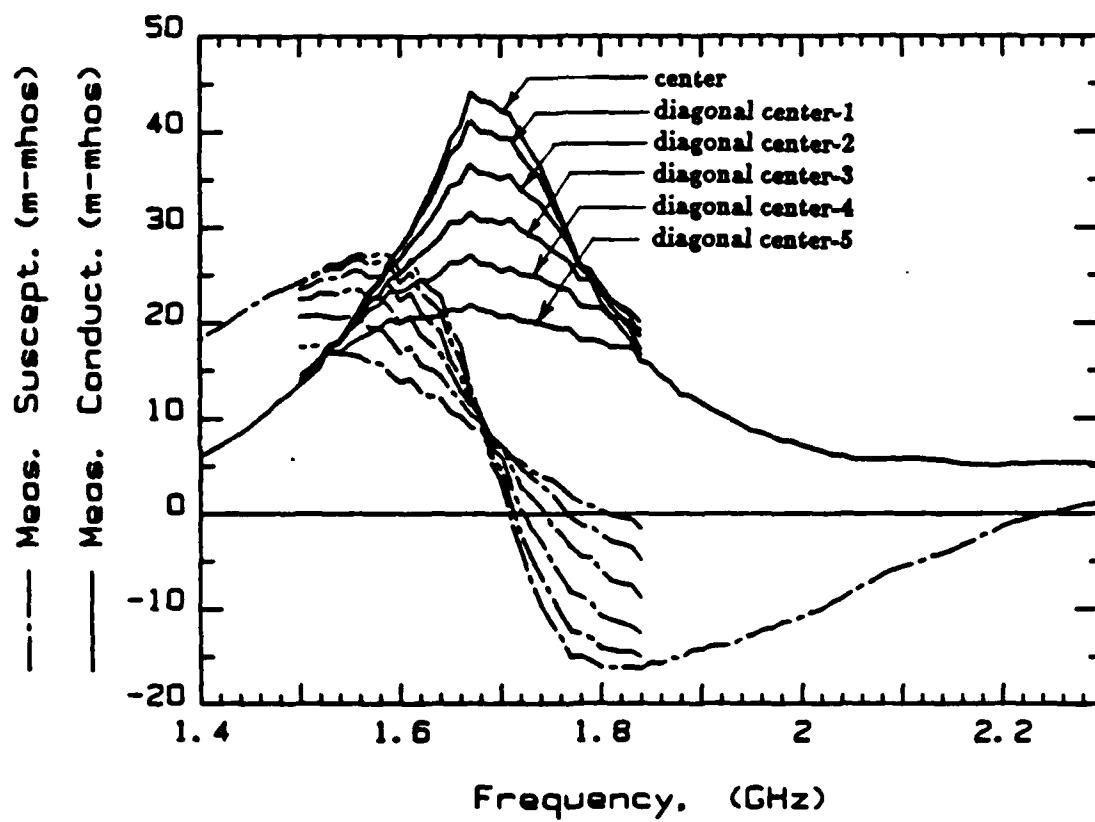


Figure C.4: 5 cm monopole on box over ground plane; feed position varies along the center-line



4 cm monopole on box over ground plane

Figure C.5: 4 cm monopole on box over ground plane; feed position varies along the diagonal

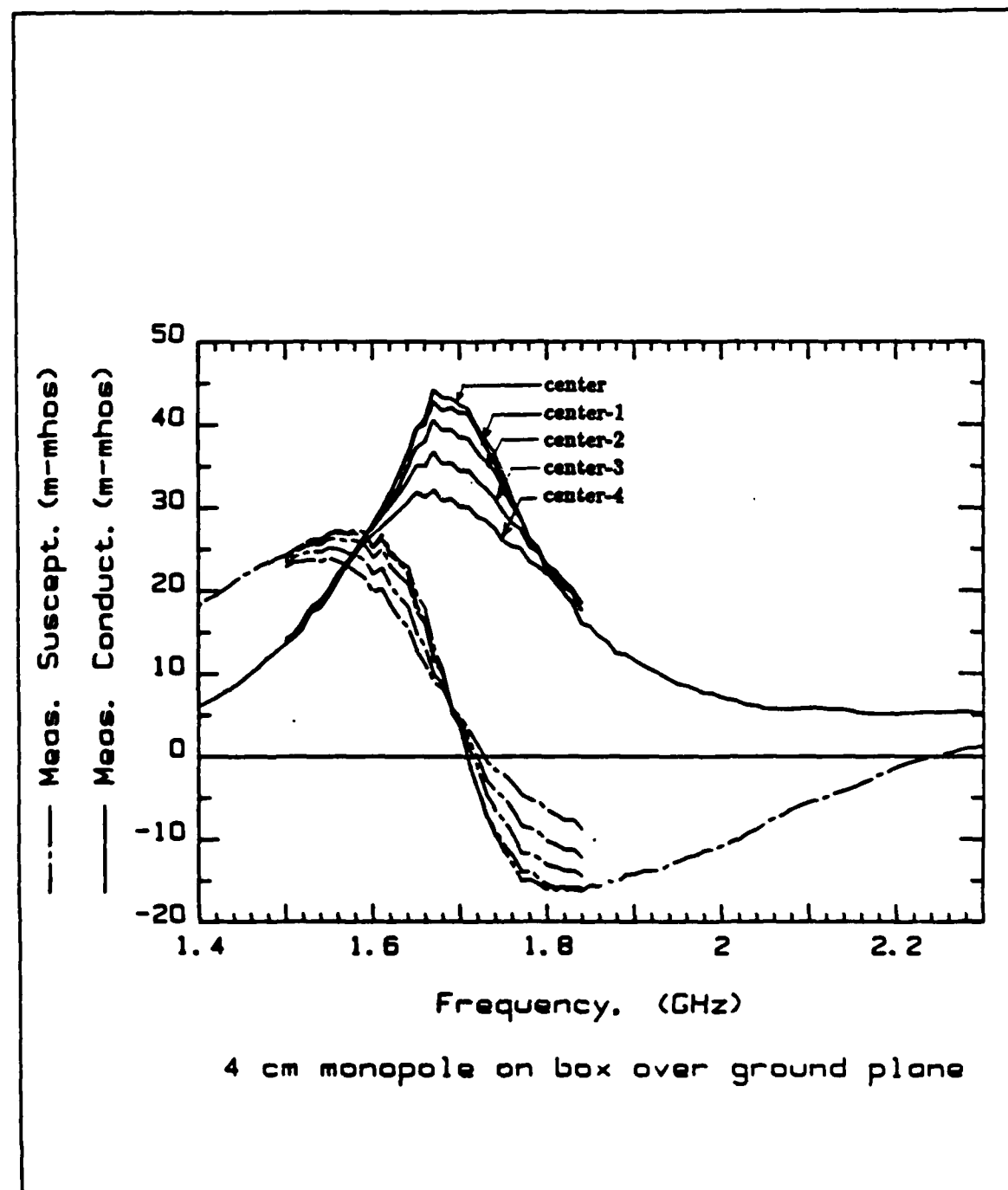
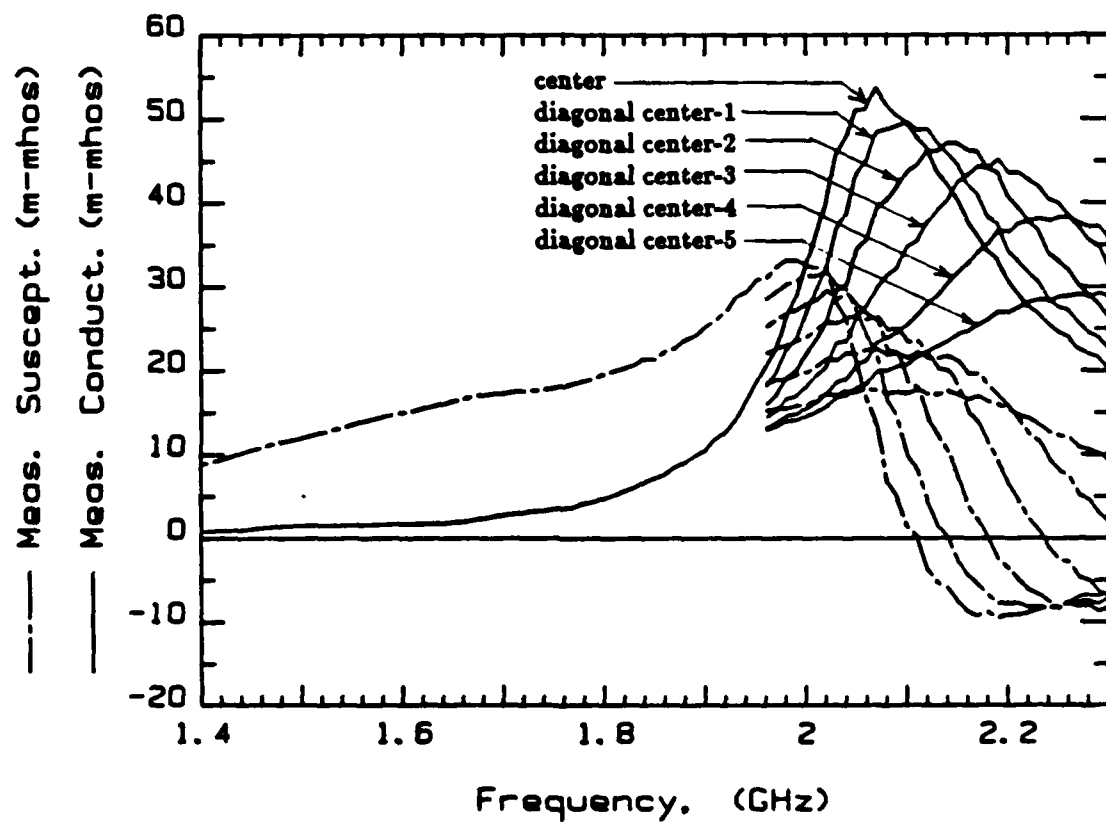
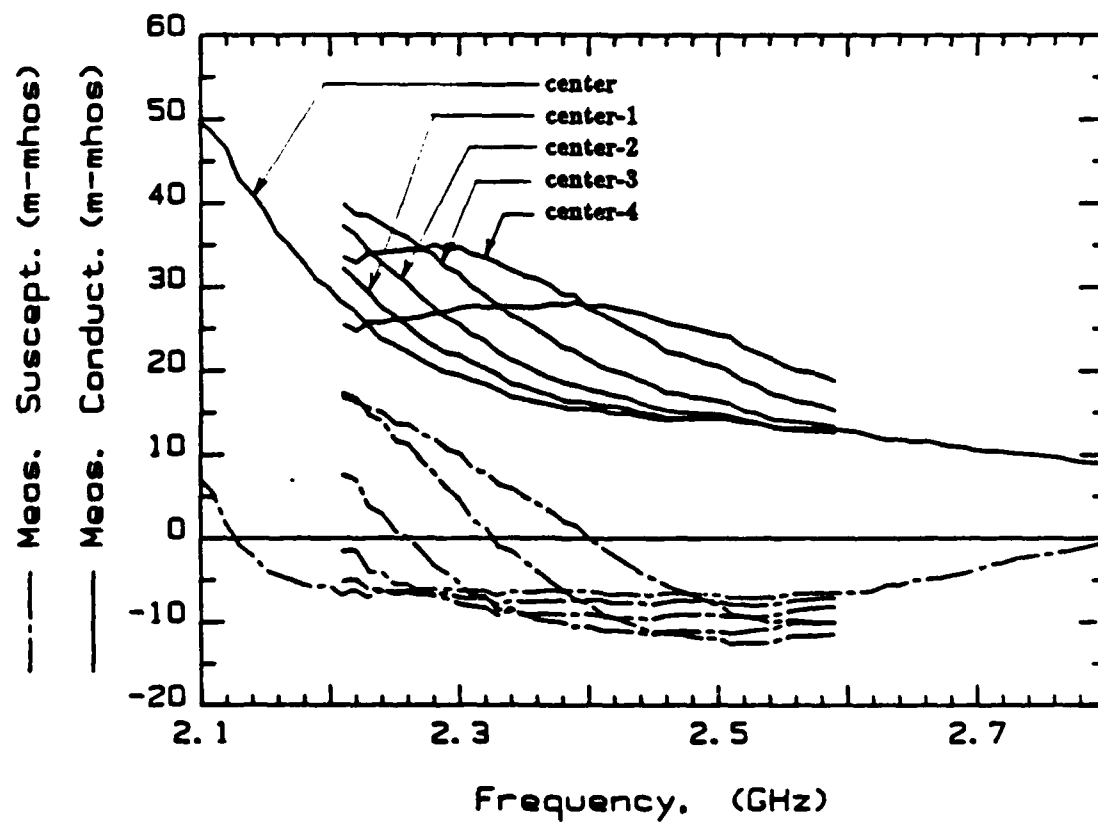


Figure C.6: 4 cm monopole on box over ground plane; feed position varies along the center-line



3 cm monopole on box over ground plane

Figure C.7: 3 cm monopole on box over ground plane; feed position varies along the diagonal



3 cm monopole on box over ground plane

Figure C.8: 3 cm monopole on box over ground plane; feed position varies along the center-line



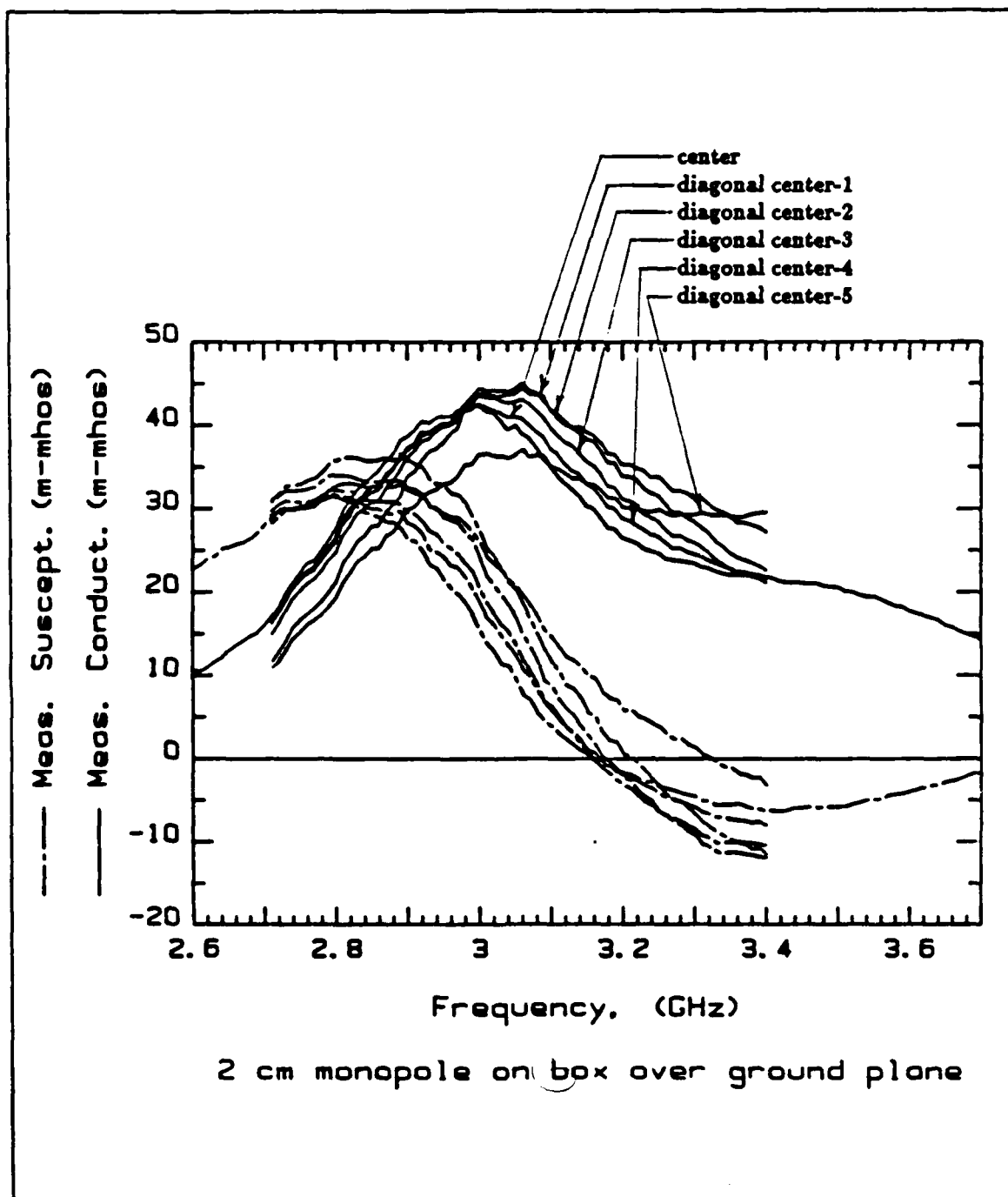


Figure C.9: 2 cm monopole on box over ground plane; feed position varies along the diagonal

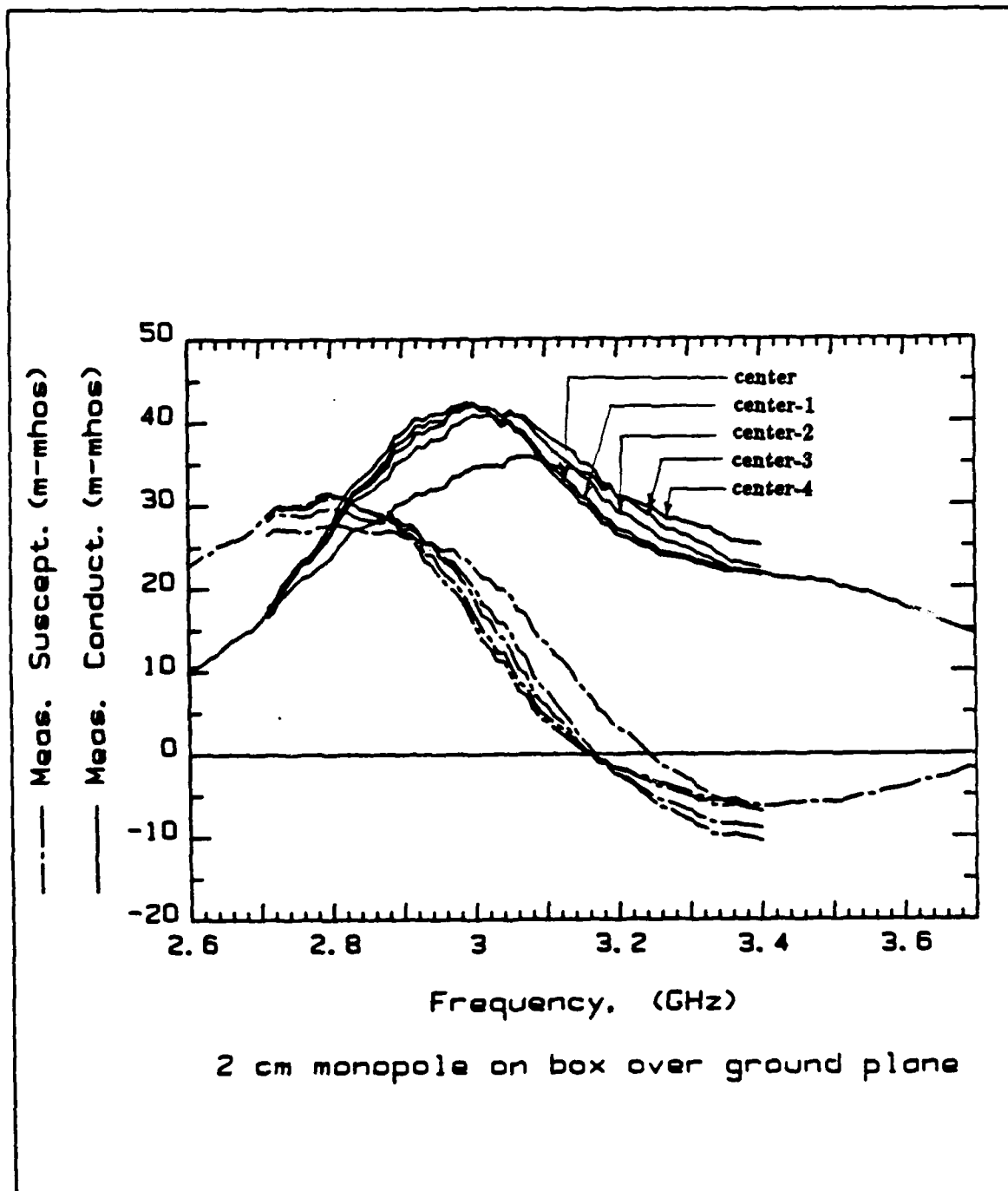


Figure C.10: 2 cm monopole on box over ground plane; feed position varies along the center-line

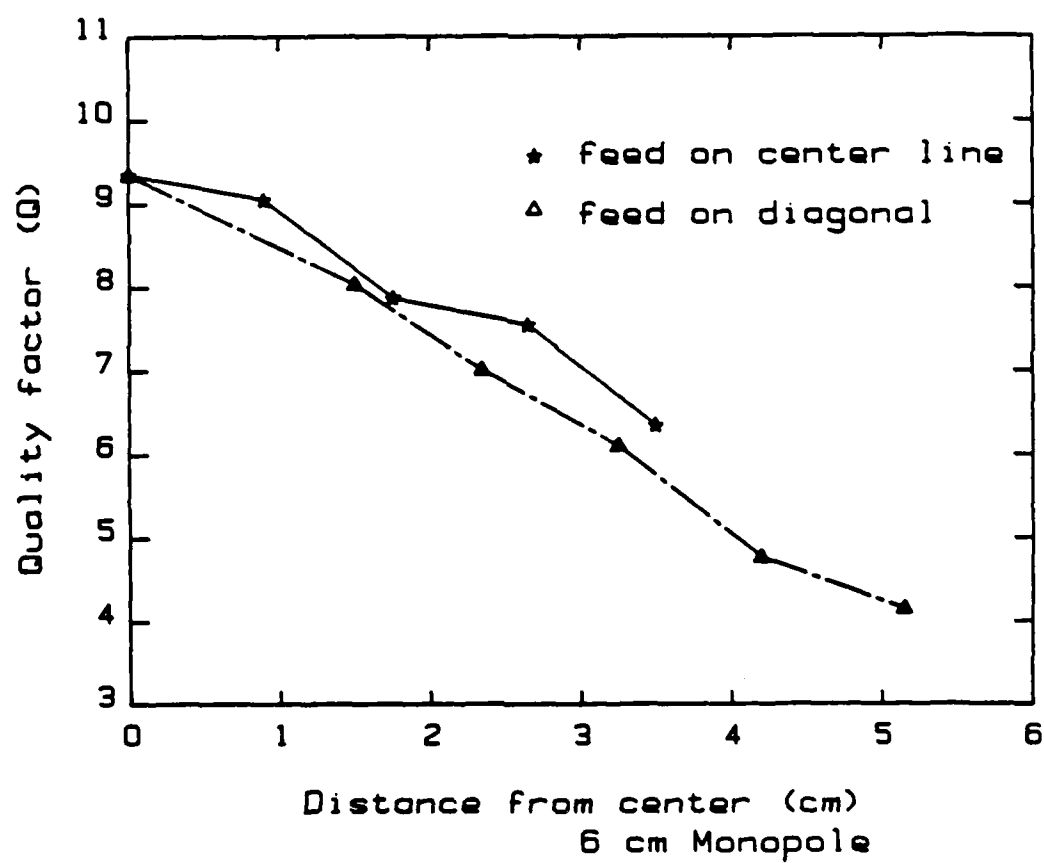


Figure C.11: Quality factor versus distance from center; 6 cm monopole

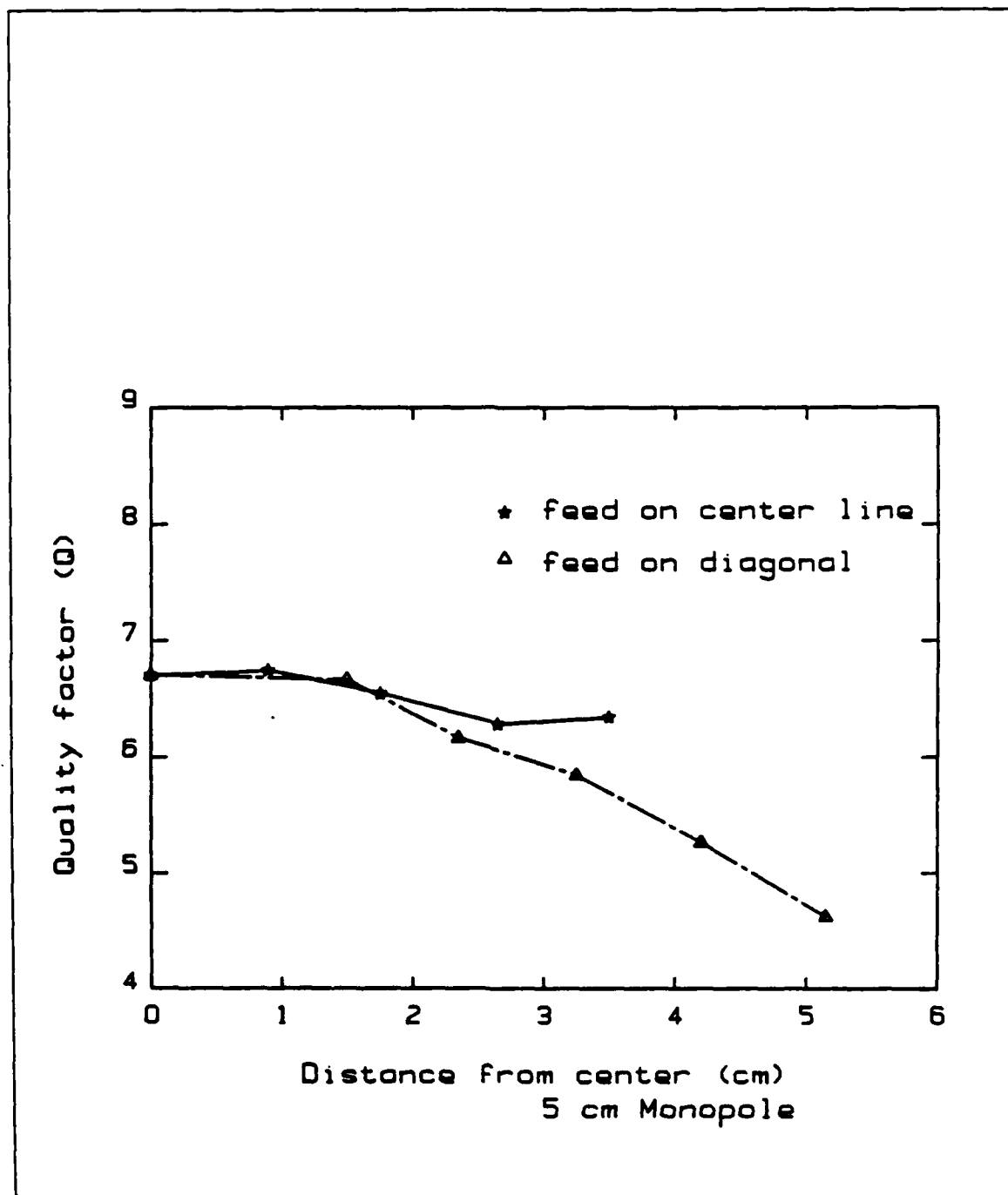


Figure C.12: Quality factor versus distance from center; 5 cm monopole

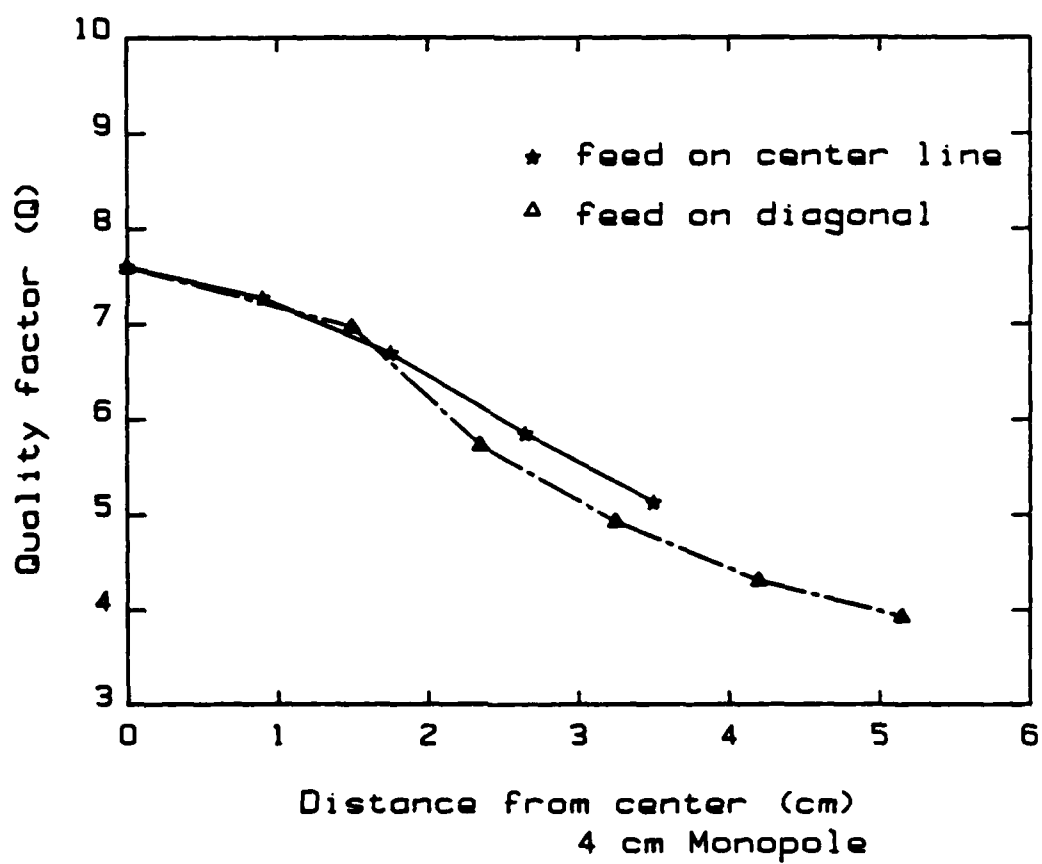


Figure C.13: Quality factor versus distance from center; 4 cm monopole

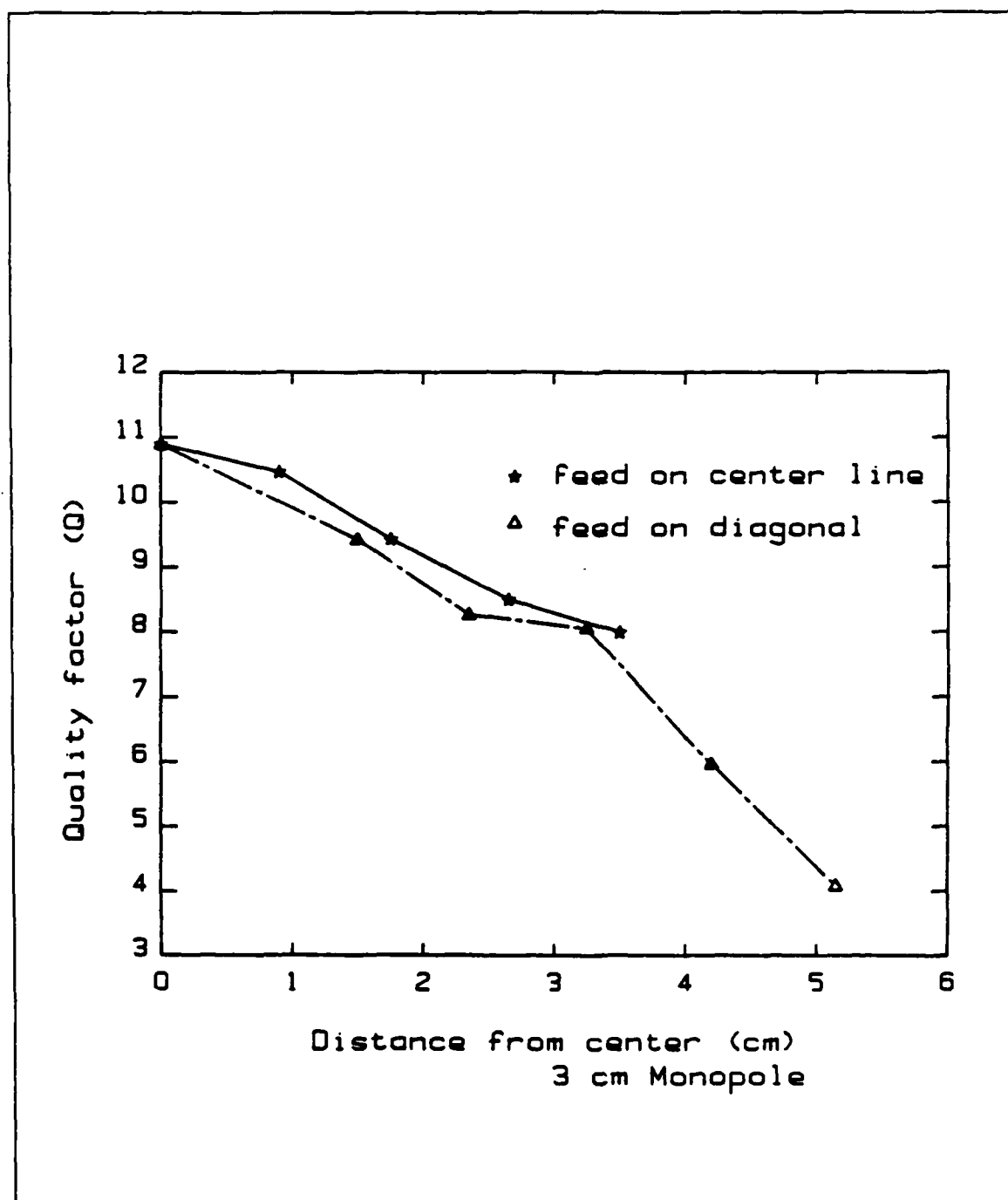


Figure C.14: Quality factor versus distance from center, 3 cm monopole

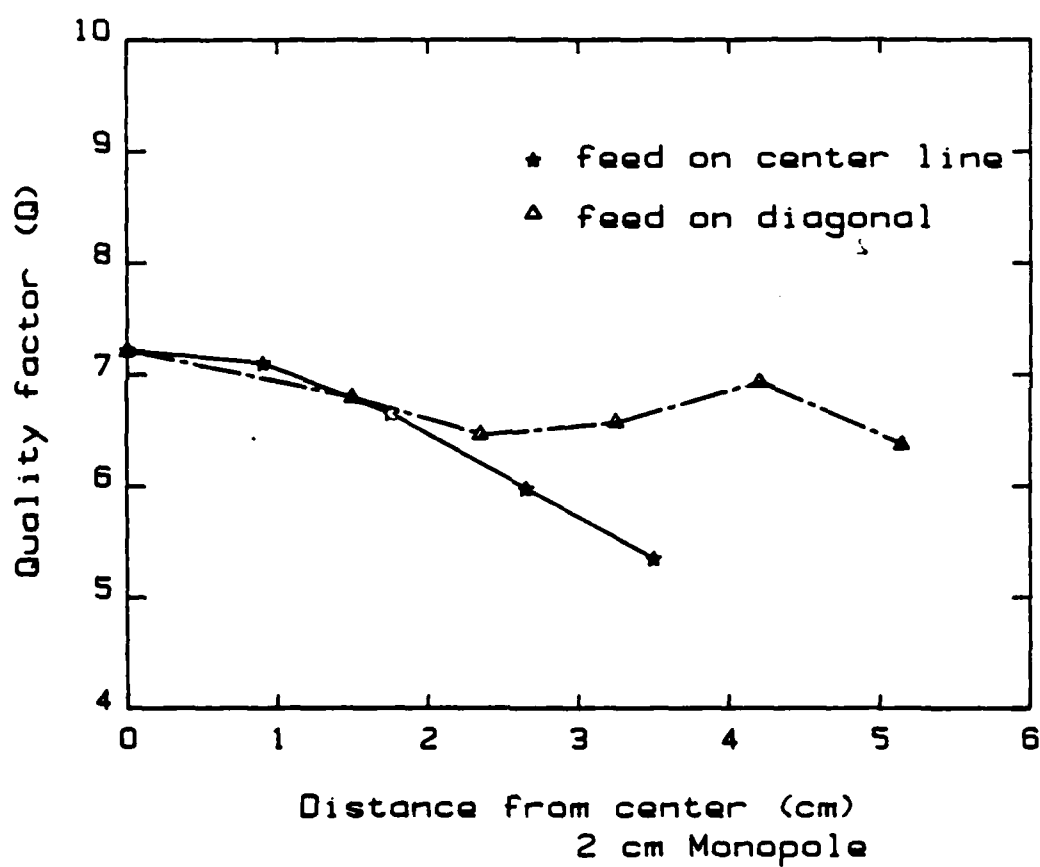


Figure C.15: Quality factor versus distance from center; 2 cm monopole

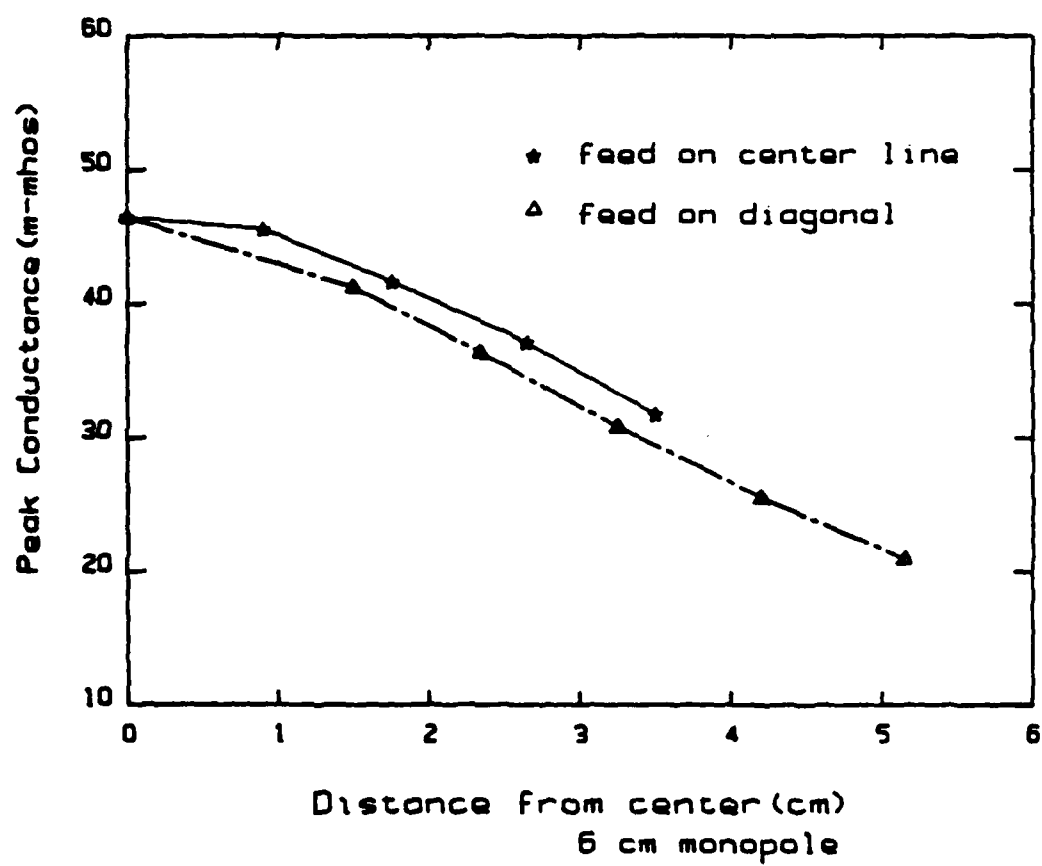


Figure C.16: Peak conductance versus distance from center; 6 cm monopole



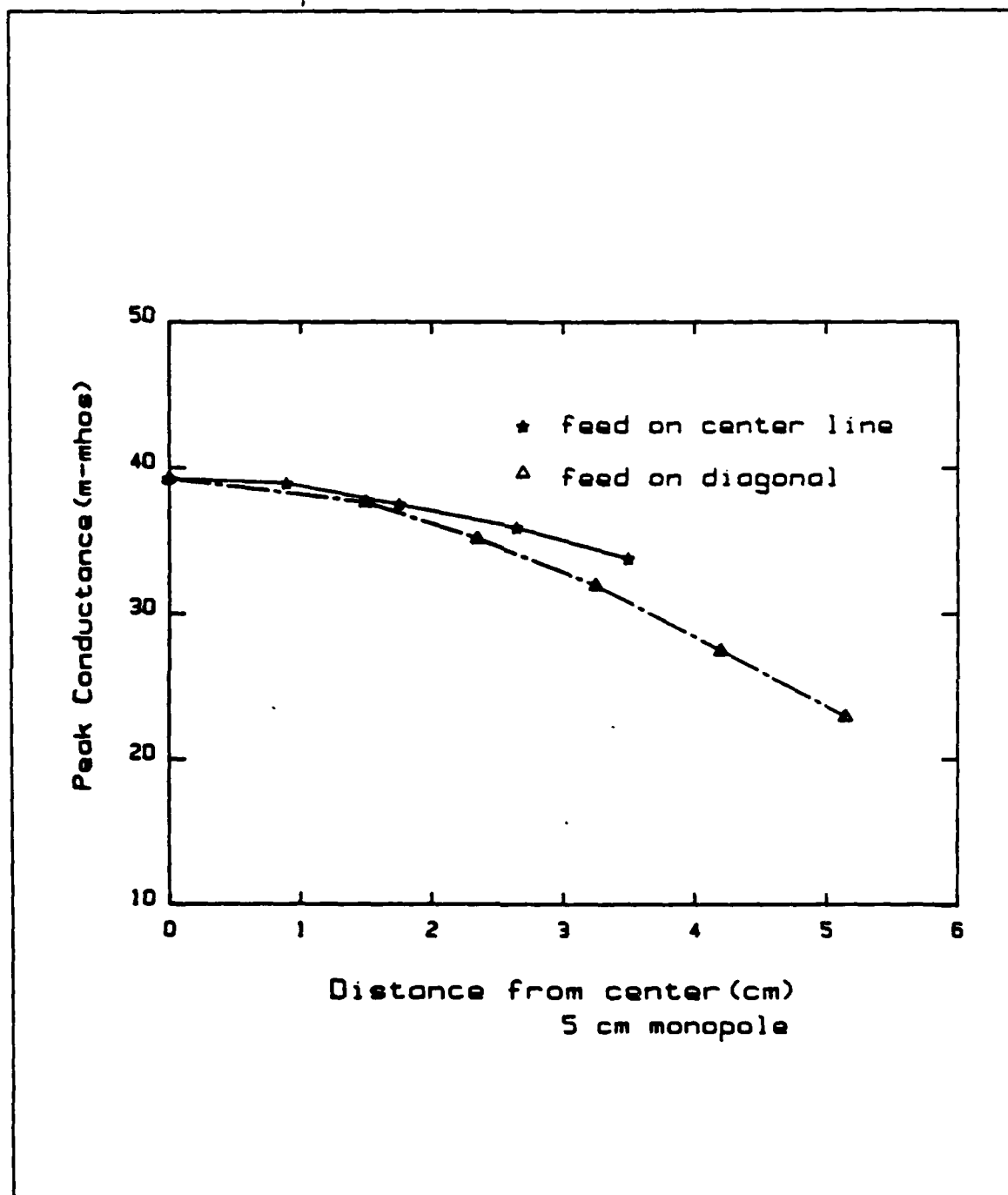


Figure C.17: Peak conductance versus distance from center; 5 cm monopole

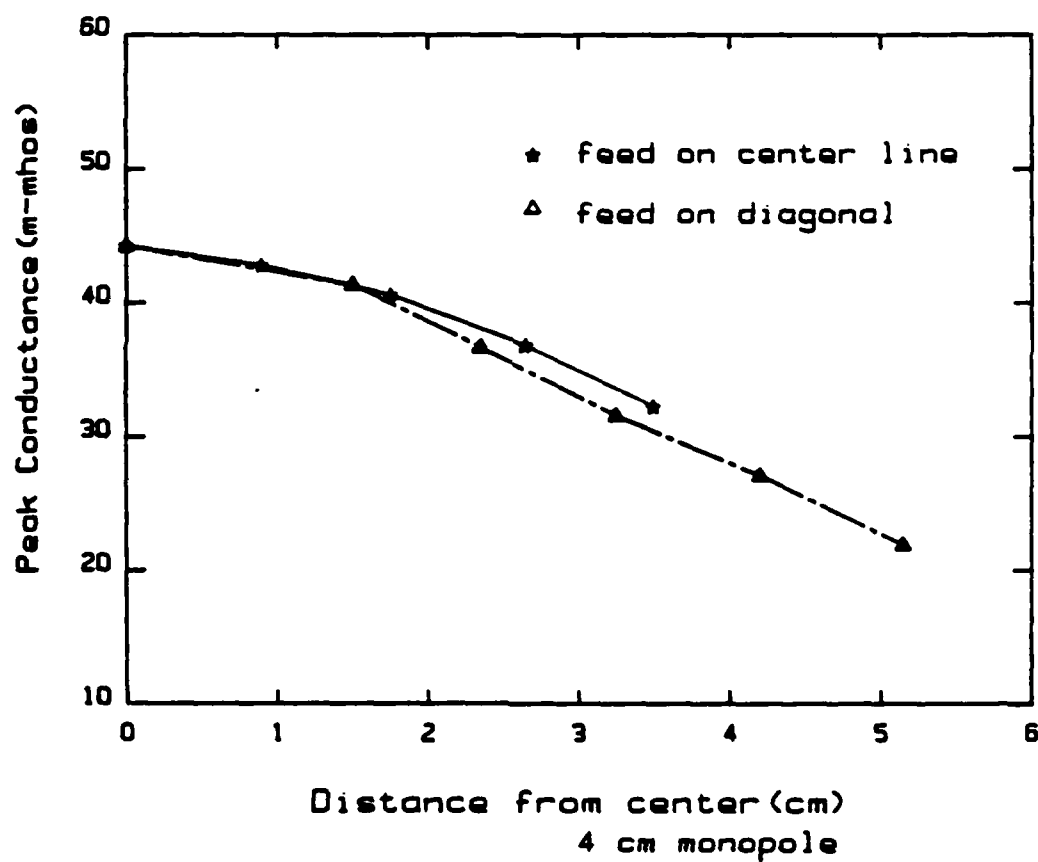


Figure C.18: Peak conductance versus distance from center; 4 cm monopole

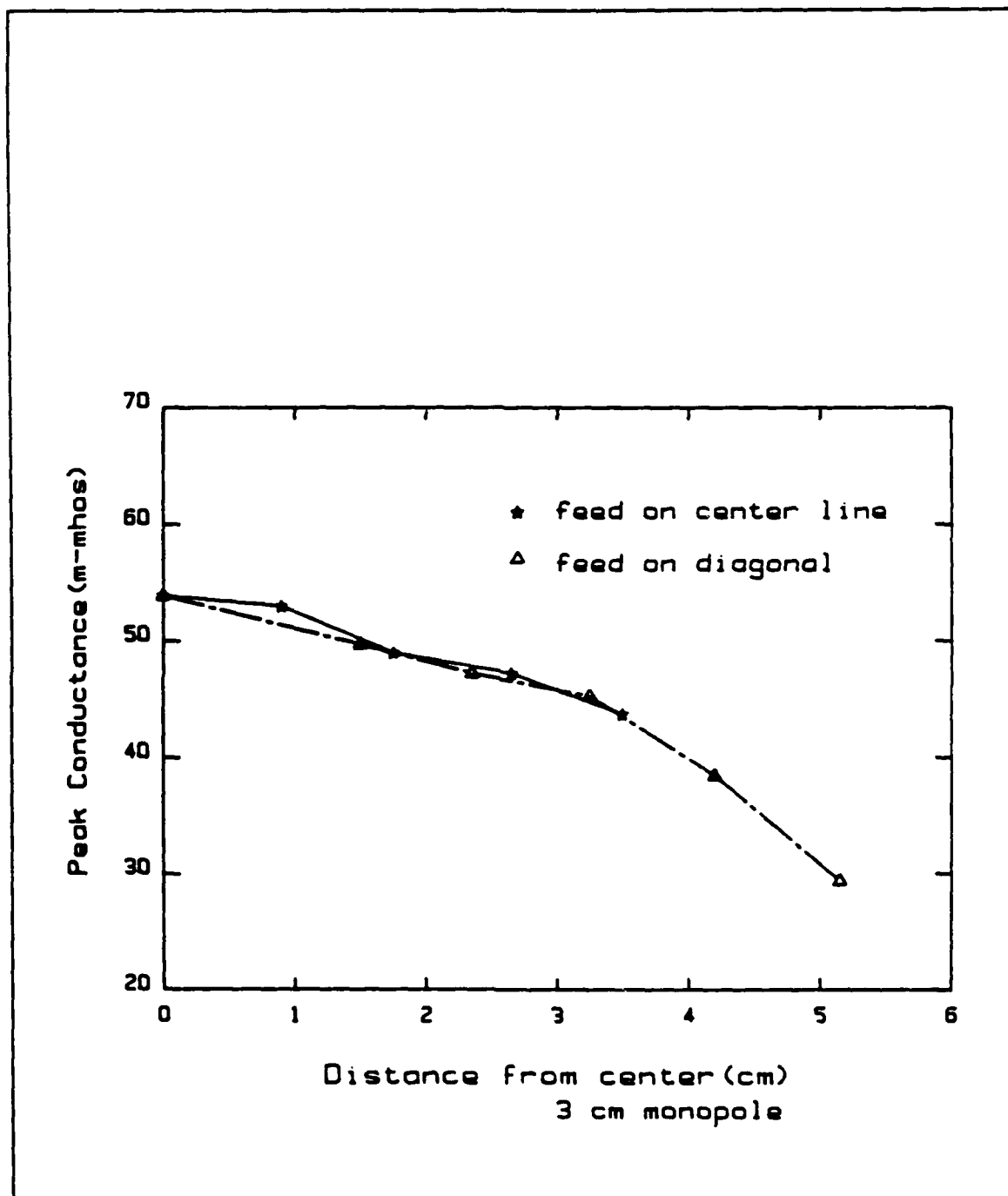


Figure C.19: Peak conductance versus distance from center, 3 cm monopole

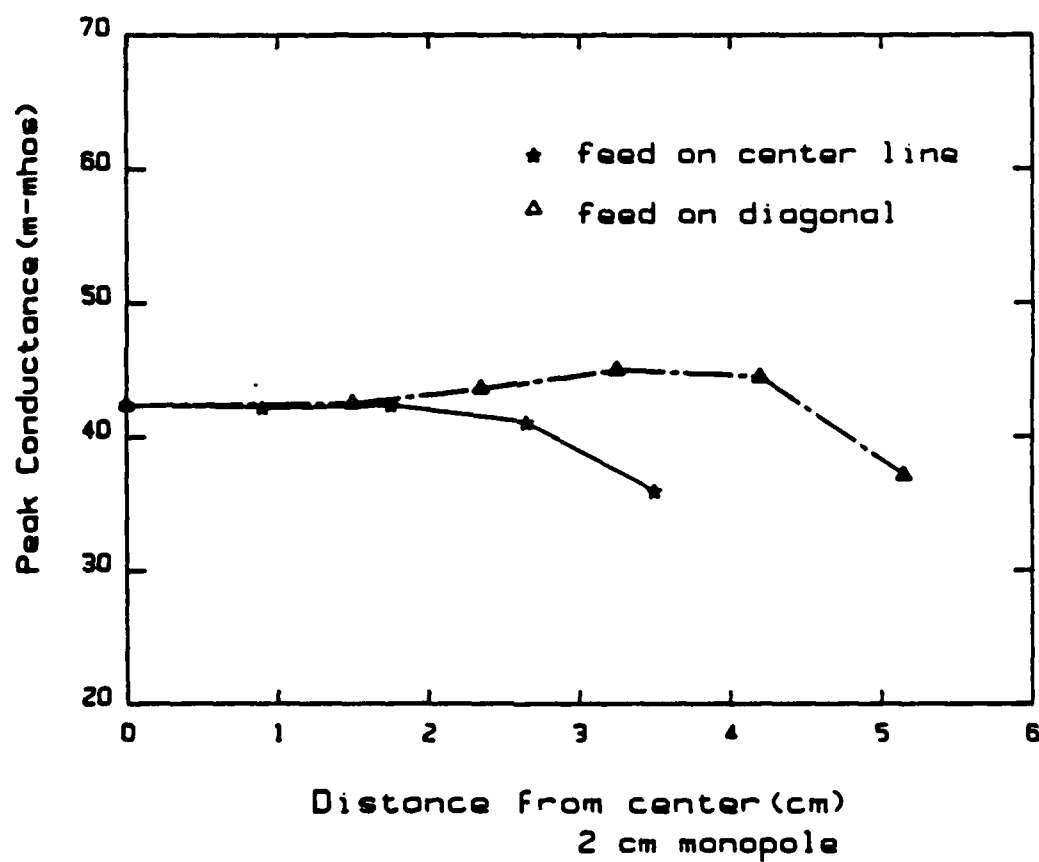


Figure C.20: Peak conductance versus distance from center; 2 cm monopole

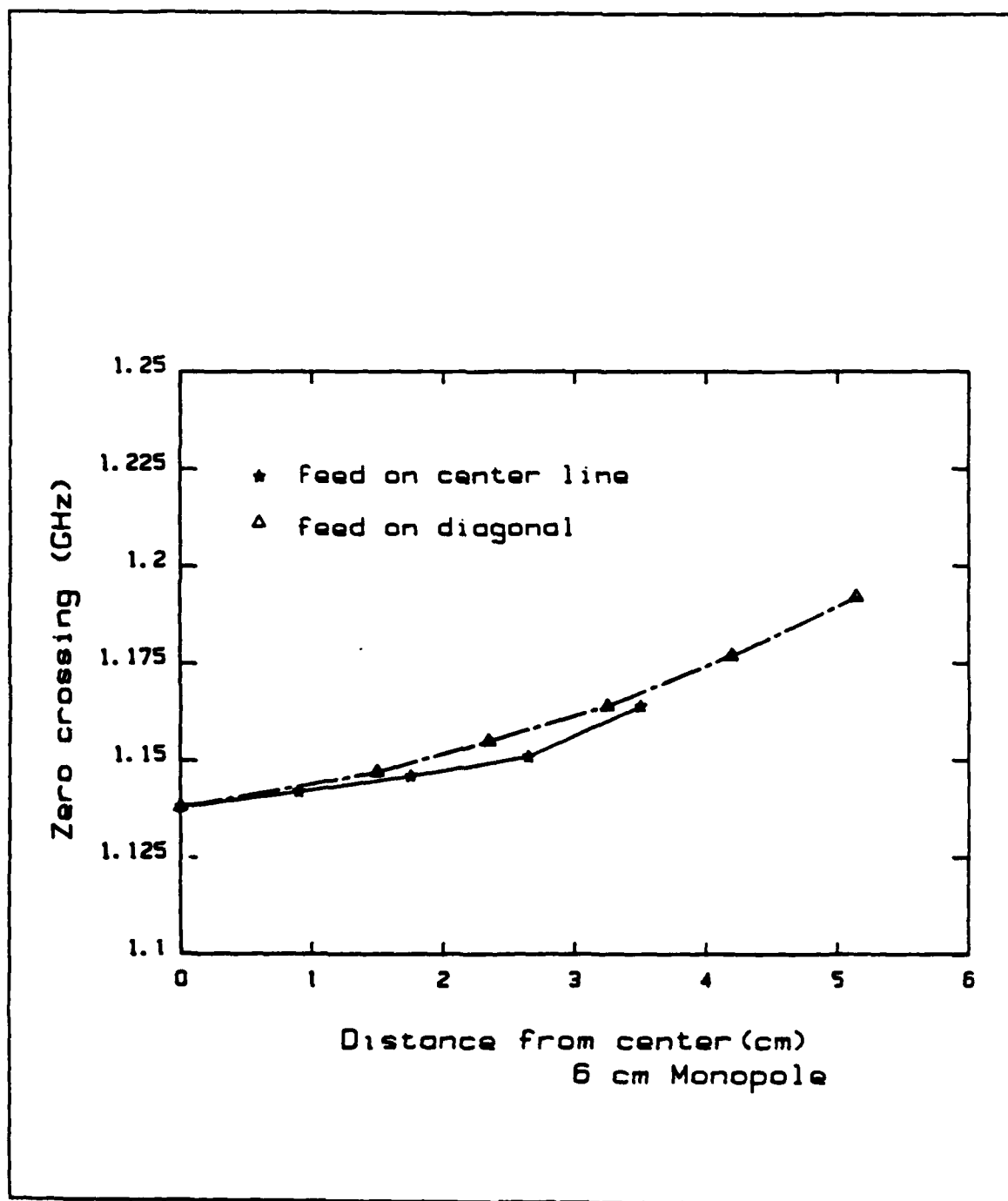


Figure C.21: Zero crossing frequency versus distance from center; 6 cm monopole

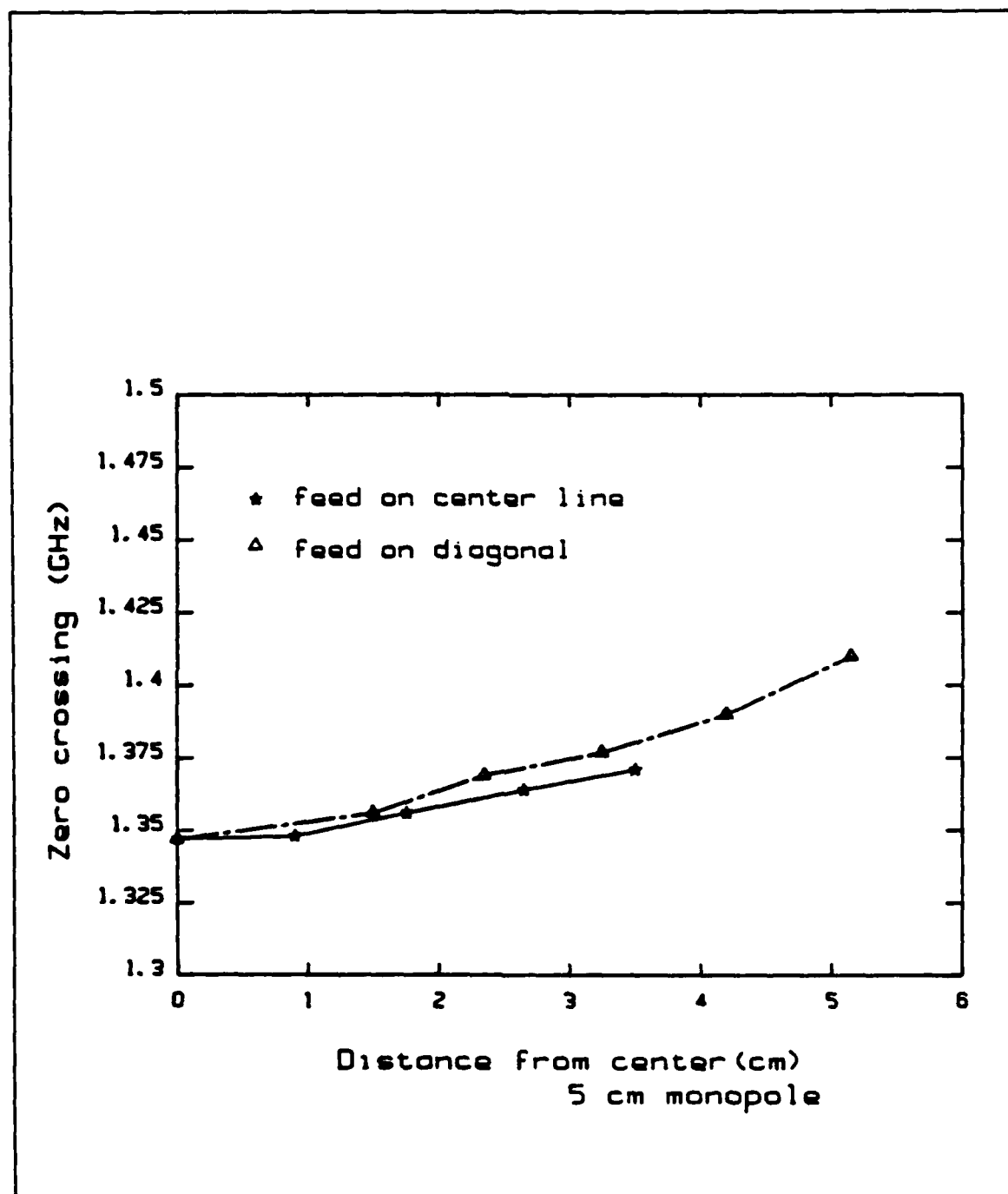


Figure C.22: Zero crossing frequency versus distance from center; 5 cm monopole

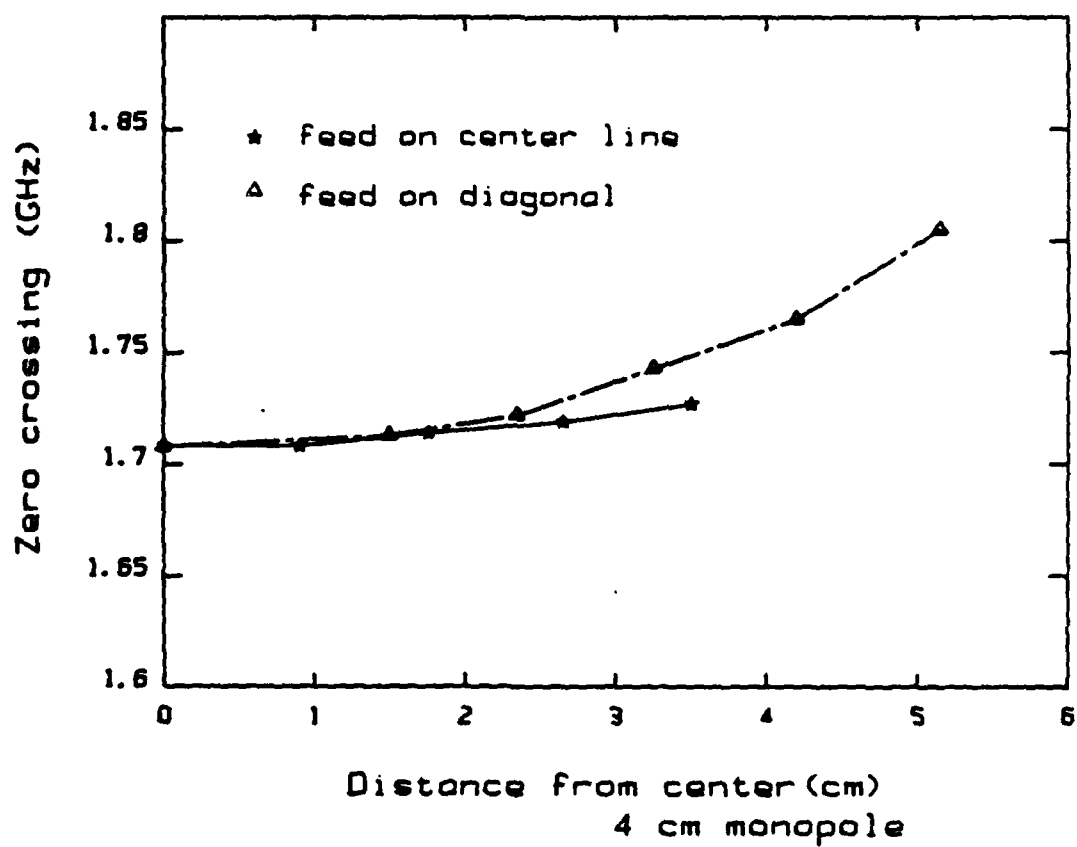


Figure C.23: Zero crossing frequency versus distance from center; 4 cm monopole

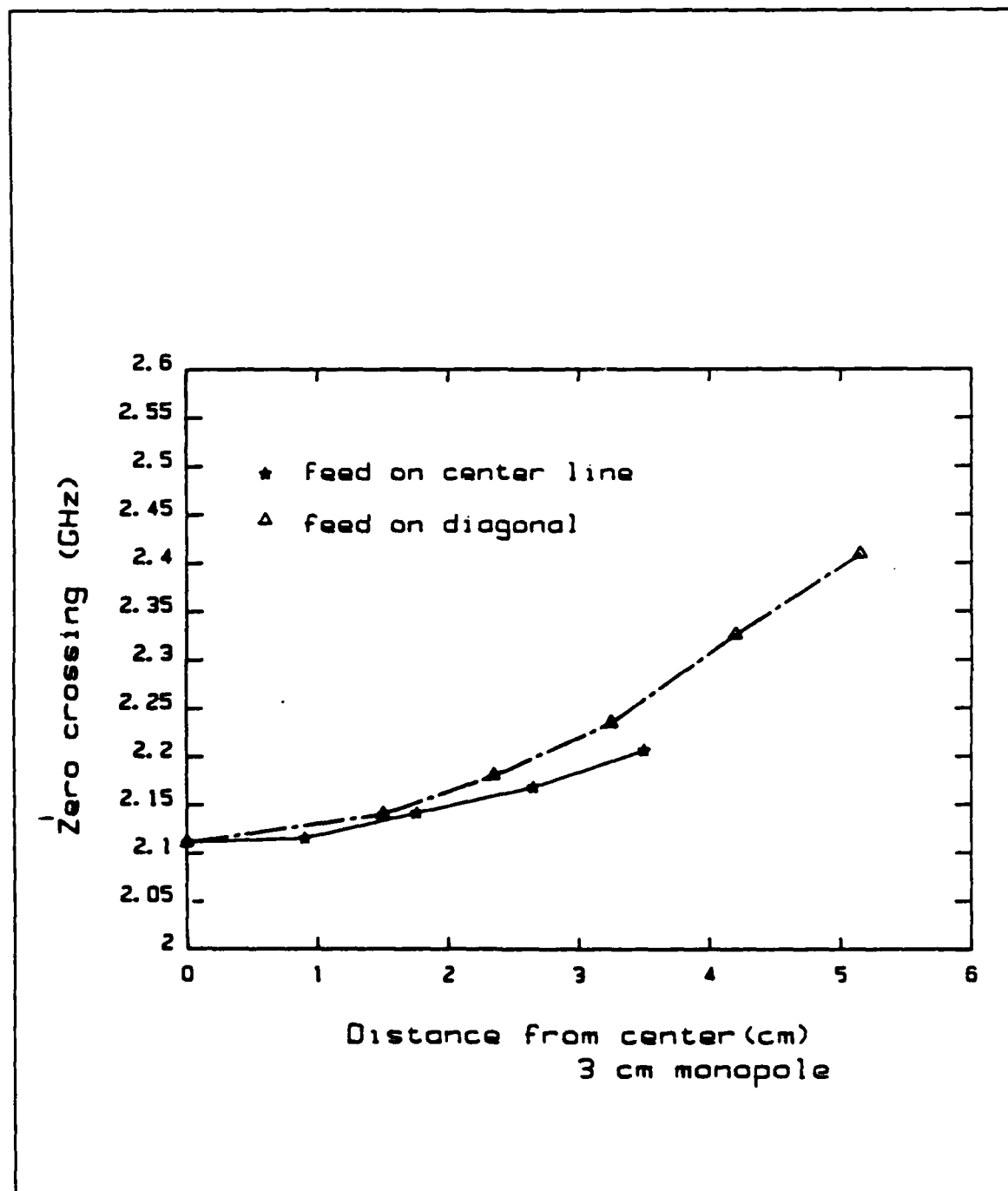


Figure C.24: Zero crossing frequency versus distance from center, 3 cm monopole



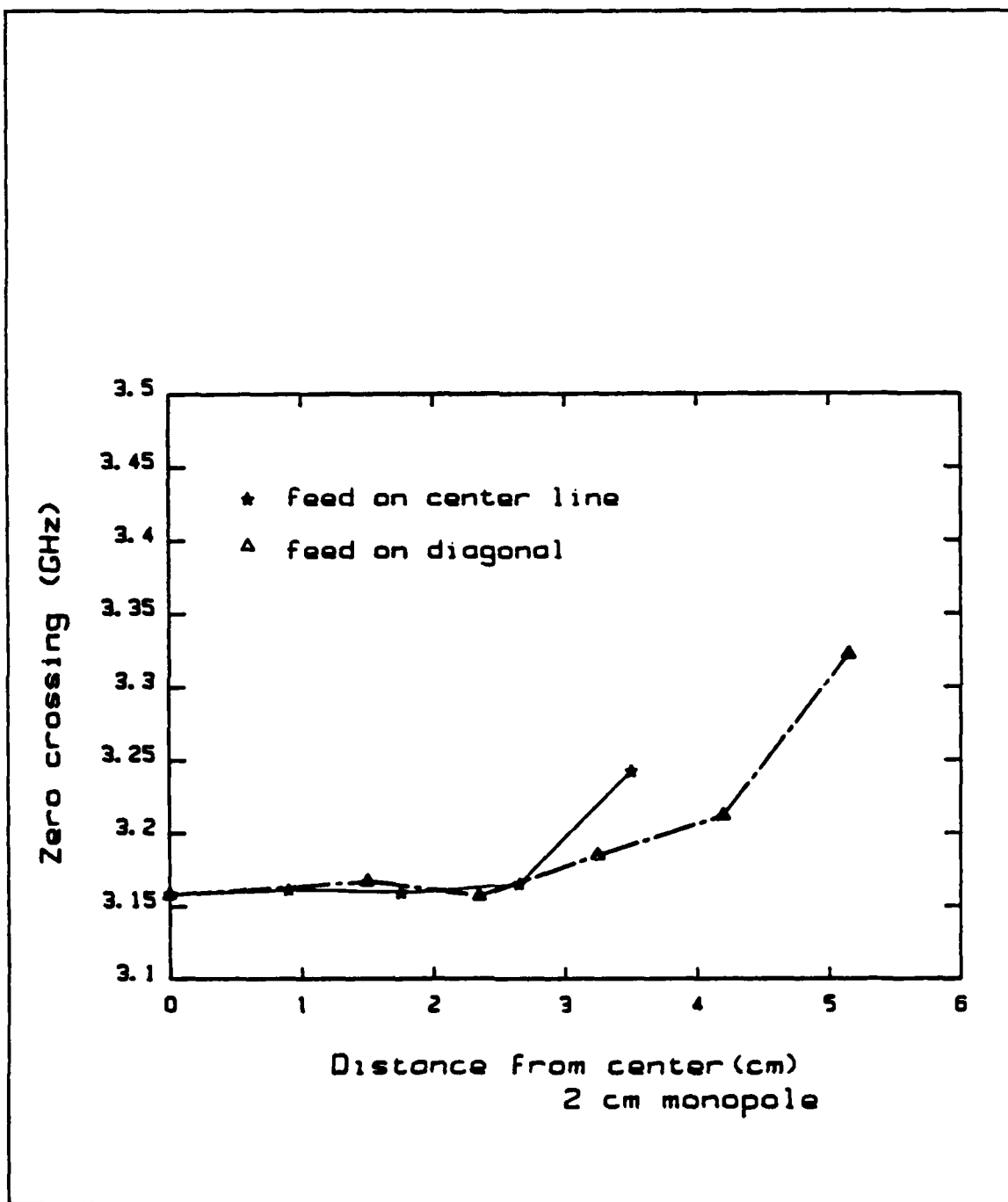


Figure C.25: Zero crossing frequency versus distance from center; 2 cm monopole

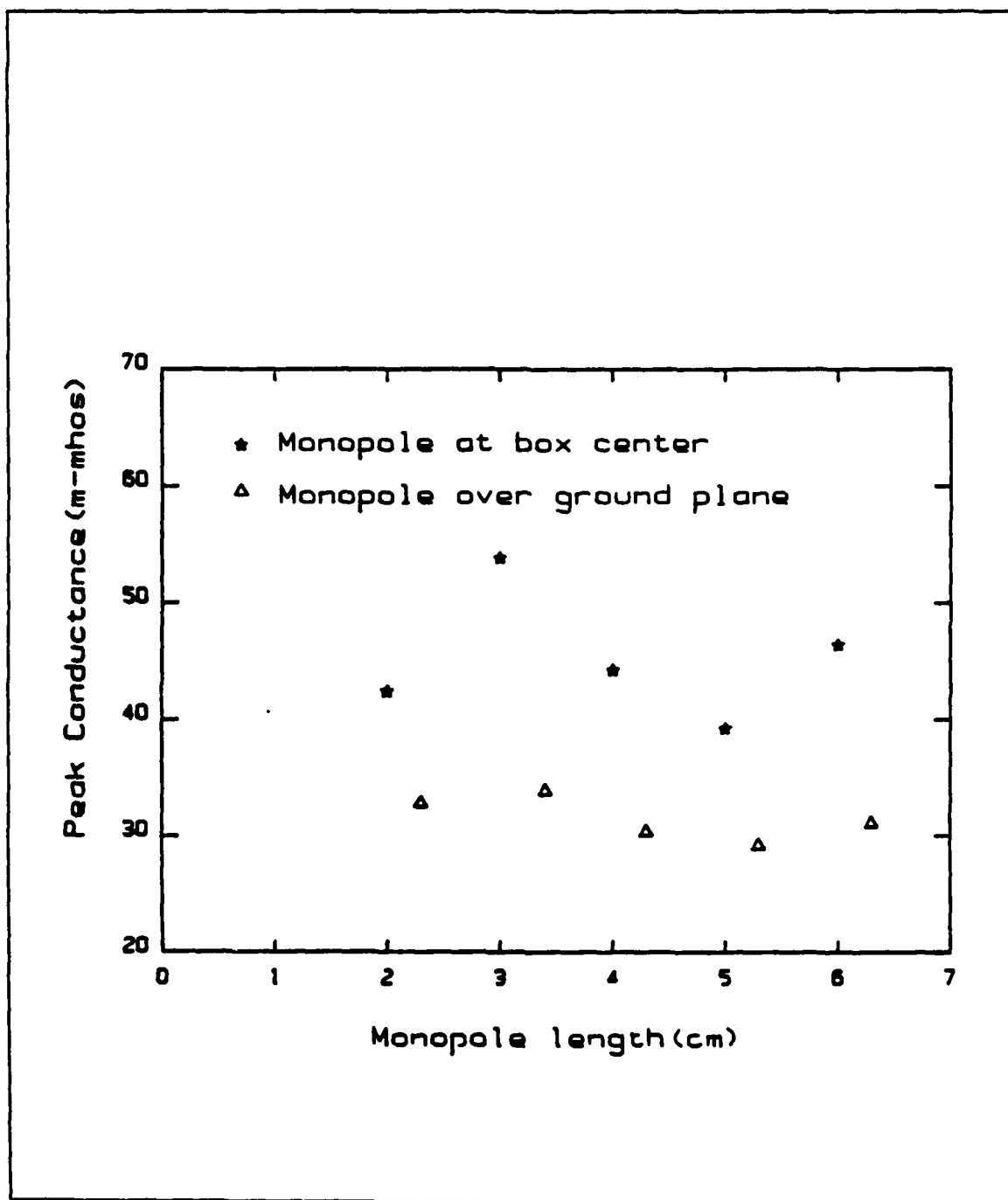


Figure C.26: Peak conductance versus monopole length

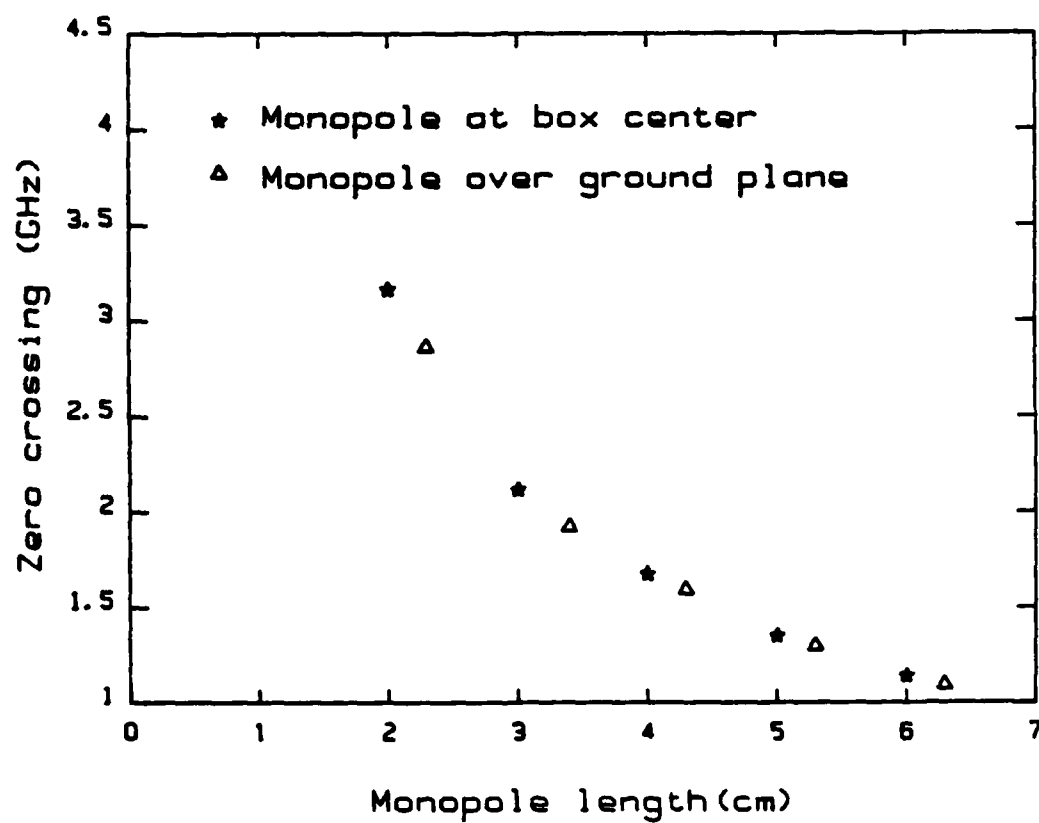


Figure C.27: Zero crossing frequency versus monopole length

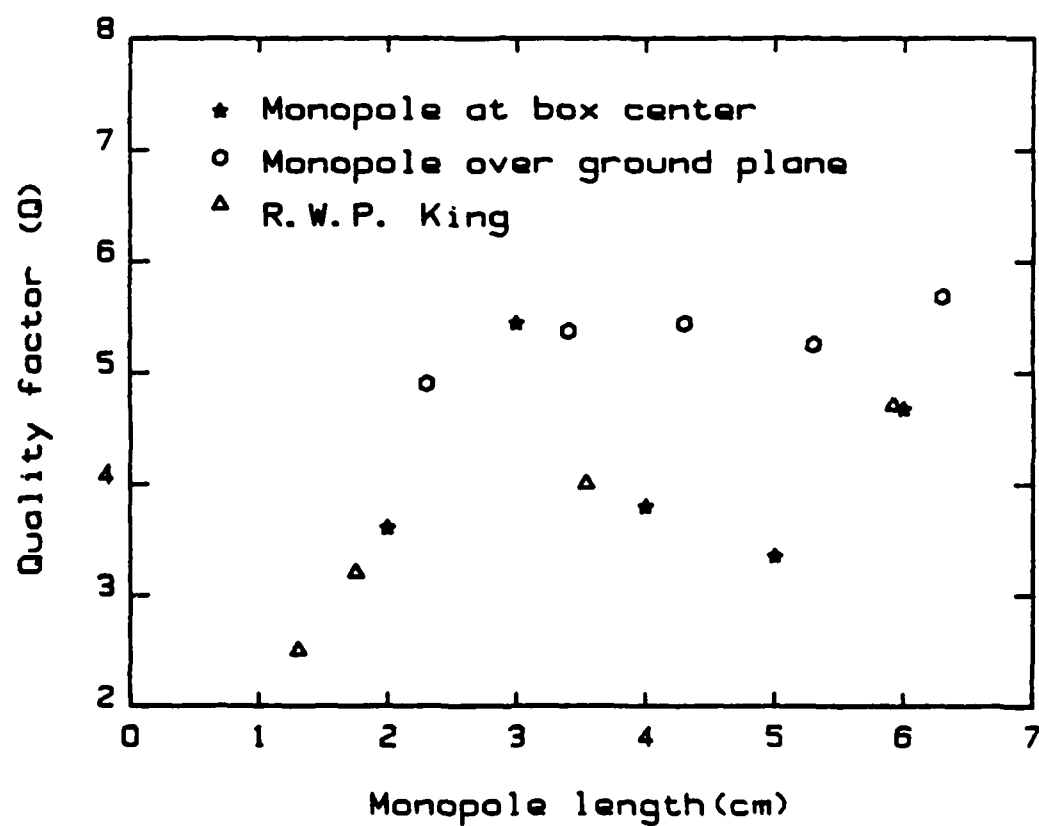


Figure C.28: Quality factor versus monopole length

## Appendix D

# Numerical Analysis

Rao, Wilton and Glisson [4] introduced a method to find the surface currents on a scatterer using the electric field integral equation and triangular patch modeling. The scattered electric field  $\mathbf{E}^s$  can be computed from the surface currents by

$$\mathbf{E}^s = -j\omega\mathbf{A} - \nabla\Phi$$

where  $\mathbf{A}$  is the magnetic vector potential defined as

$$\mathbf{A}(\mathbf{r}) = \frac{\mu}{4\pi} \int_S \mathbf{J} \frac{e^{-jkR}}{R} dS'$$

and the scalar potential is

$$\Phi(\mathbf{r}) = \frac{1}{4\pi\epsilon} \int_S \sigma \frac{e^{-jkR}}{R} dS'; \quad R = |\mathbf{r} - \mathbf{r}'|$$

where  $\sigma$  is the surface charge density,  $\mathbf{J}$  is the surface current density,  $\mathbf{r}$  is the distance to observation point and  $\mathbf{r}'$  is the distance to source point. Using the continuity equation one obtains

$$\nabla_s \cdot \mathbf{J} = -j\omega\sigma$$

By applying the boundary condition

$$\hat{n} \times (\mathbf{E}^i + \mathbf{E}^s) = 0 \quad \text{on } S$$

where  $\hat{n}$  is the unit normal to the patch, one obtains

$$\mathbf{E}_{tan}^i = (-j\omega\mathbf{A} - \nabla\Phi)_{tan} ; \quad \mathbf{r} \text{ on } S$$

The surface of the scatterer is divided into triangular patches and the currents on  $S$  are approximated by the expansion functions  $\mathbf{F}_n$  as

$$\mathbf{J} = \sum_{n=1}^N I_n \mathbf{F}_n(\mathbf{r})$$

where  $n$  is the number of interior edges. Application of Galerkins' technique results in

$$\langle \mathbf{F}_m, \mathbf{E}^i \rangle = - \langle \mathbf{F}_m, \mathbf{E}^{inc} \rangle ; \quad m = 1, \dots, N$$

from which results a linear system of equation which may be solved for the current coefficients  $I_n$ . To implement the numerical technique, the box was divided into triangular patches. Since the current at the base of the monopole is a maximum, the region around the base of the monopole is divided into smaller triangular patches than the region much further away from the monopole. This triangular patch model of the box and the monopole antenna are shown in Figures D.1 through D.3. Using symmetry, only half of the box was modelled to reduce the number of unknown currents through the triangular patch edges. A perfect magnetic conducting plane was assumed at this plane of symmetry. For the monopole position at the box center and at the center of an edge, the symmetry plane passes through the line connecting the center of the box to the center of an edge dividing the box in half. The wire antenna was modelled as a tape subdivided into triangular patches. The width of the tape is 0.32 cm which is approximately four times the radius of the wire antenna [5, p. 20]. A perfect electric conducting plane was assumed at the base of the box to model the ground plane on which the box was mounted.

This triangular patch model of the box resulted in 97 vertices, 251 edges and 155 faces. The average edge length of the triangular patches was 2.05 cm. The voltage

source was applied at the junction between the tape and the top surface of the box which was designated as edge number 152 when the monopole was at the box center and edge number 144 when the monopole was at the box edge. Figure D.1 shows a perspective views of half of the box when the monopole is at the center of the box. Figure D.2 shows the triangular patch of the model of half of the box with the monopole at the feed position nearest to the edge of the box. The overall model of the box and the antenna was generated in the computer using a 'BUILD' code that was developed by Dr. Bill Johnson of Sandia National Laboratory. These results were then used as the input data for another computer program called PATCH to determine the currents flowing through the interior edges of the triangular patches. Since a unit voltage source was applied at the junction, the current flowing through the base of the tape was the input admittance for the specified frequency.

A completely different model of the box had to be generated for the case in which the monopole was located at the box corner to take advantage of the new plane of symmetry which was now along a line joining the center of the box to the corner of the box. A sketch of this new model is shown in Figure D.3. A perfect magnetic conducting plane was specified at this plane of symmetry and a perfect electric conducting plane was specified at the base of the box to account for the ground plane. There were 104 vertices, 269 edges and 166 faces. The maximum edge length was 2.86 cm. A unit voltage source was applied at the junction between the tape and the top surface of the box at edge number 246.

The tape length was adjusted to account for the different monopole lengths. All five different lengths of monopoles were considered in the numerical analysis. For a particular length of monopole the input admittance was determined for several different frequencies in the range of interest. This whole process was repeated for different lengths of monopoles and for the two different models of the box as

mentioned above.

Figures D.4 through D.18 show the numerically calculated data points superimposed on experimental plots of admittance versus frequency for the 6 cm, 5 cm, 4 cm, 3 cm and 2 cm long monopoles. For each monopole length a comparison was made for three different positions of the monopole: at the box center ; at the box edge; and at the box corner. Figure D.4 shows the comparison between the computed and the experimental data points when the 6 cm monopole was at the box center. The agreement appears to be qualitatively very good. The zero crossing frequency of the input susceptance as obtained by numerical analysis was approximately 1.17 GHz compared to 1.14 GHz for the experimental case.

The computed value of the peak of the input conductance is almost the same as the measured value but the peak is slightly shifted to the right. Both curves qualitatively follow the same general trend. The agreement is excellent up to 1.2 GHz and then starts to show minor deviations. The agreement for the imaginary part of the input admittance is also very good for this case. When the monopole is at the feed position nearest to the box edge(Figure D.5), the agreement between the numerically calculated and experimental data is reasonably good and qualitatively follows the same general trend. Figure D.6 shows a comparison between the calculated and the experimental data for the 6 cm monopole at the box corner. The agreement for this case is excellent.

Similar comparisons are made for the 5 cm, 4 cm, 3 cm and 2 cm long monopole (Figures D.7 through D.18) at the box center, the box edge and the box corner. The agreement for these cases are not as good as the case for the 6 cm long monopole and the agreement deteriorates as the monopole length gets smaller. Among several other things, the accuracy of this numerical analysis is dependent upon the ratio of the wave-length to the largest dimension of the triangular patches. A ratio of



wavelength to largest patch dimension above 6 is considered good. As the resonant frequency increases, this ratio becomes smaller affecting the accuracy. This problem can be handled by subdividing the box into smaller triangular patches, but then the number of unknown currents through the triangular patch edges increases considerably, requiring substantially more computer time and probably a refined algorithm to solve the large system of equations.

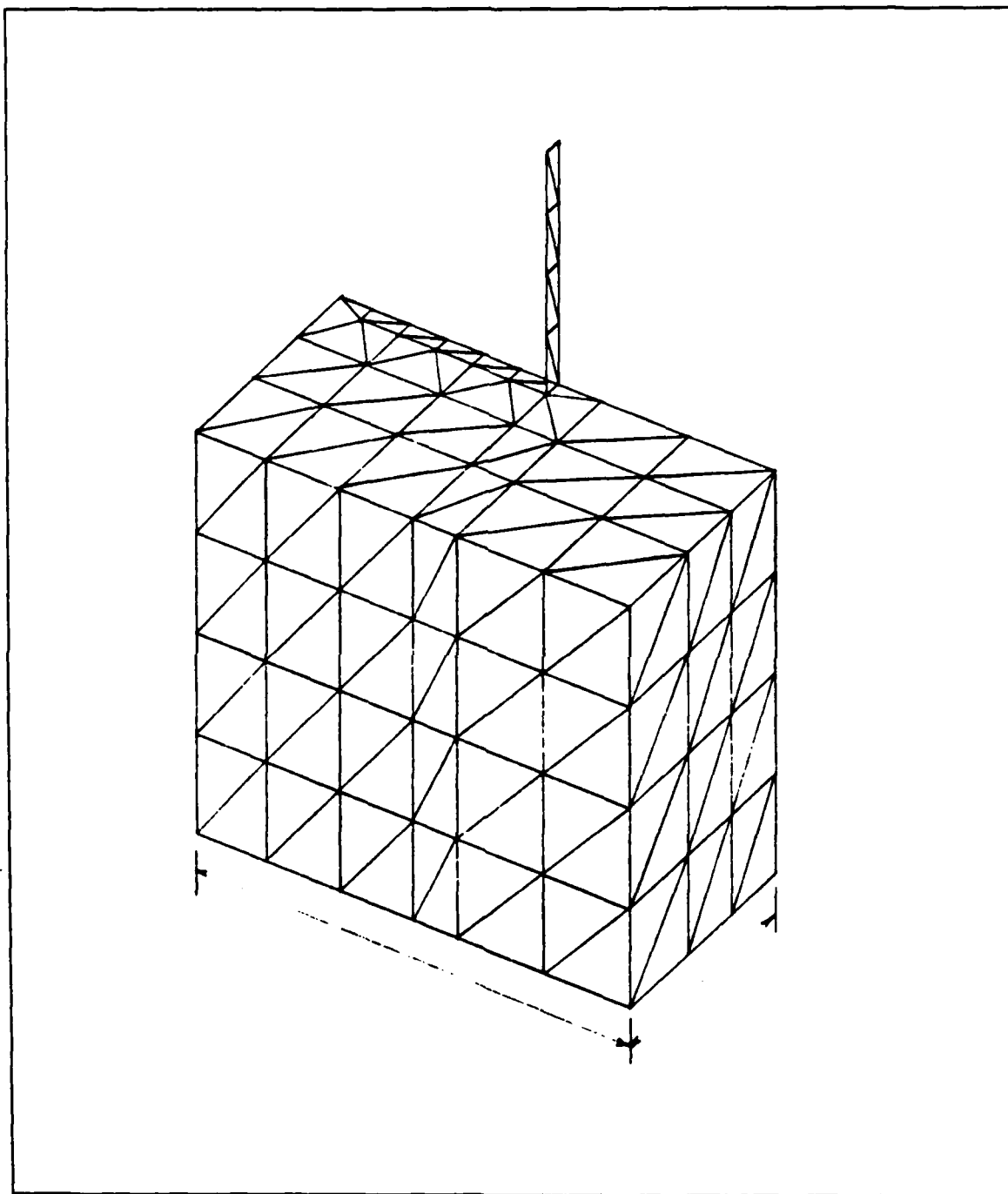


Figure D.1: Patch model; monopole at box center; front view

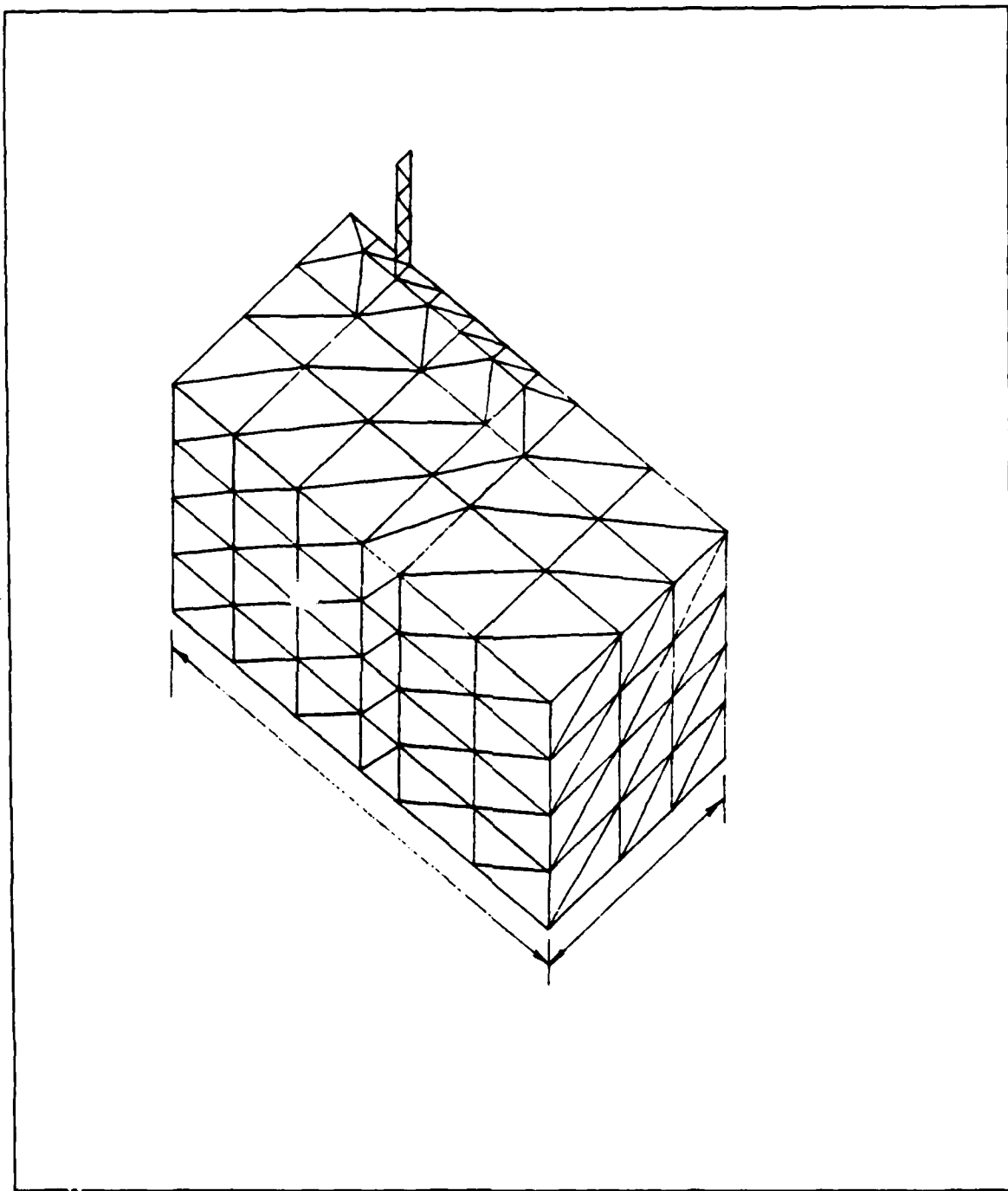


Figure D.2: Patch model; monopole at box edge; front view

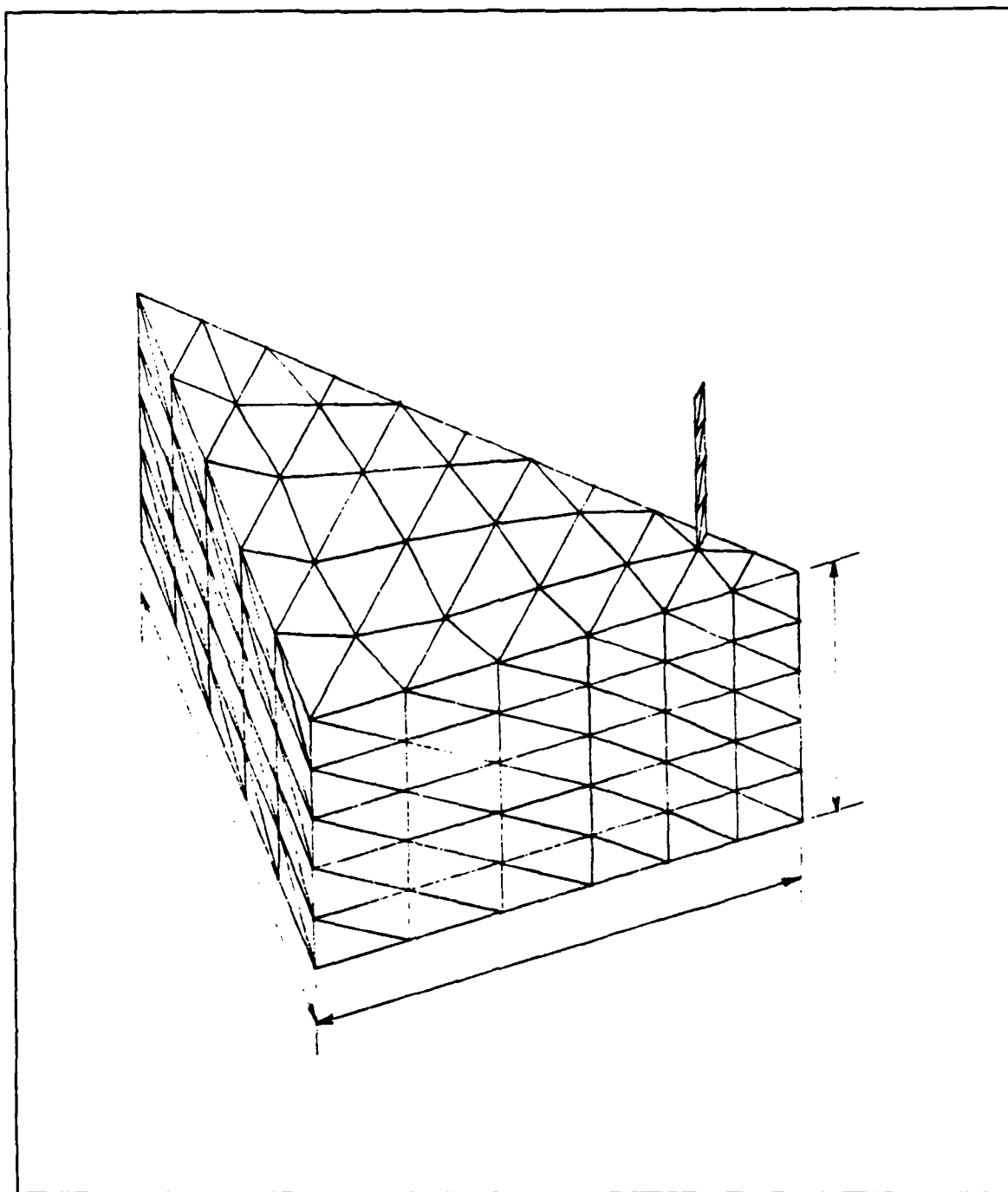


Figure D.3: Patch model; monopole at box corner; front view

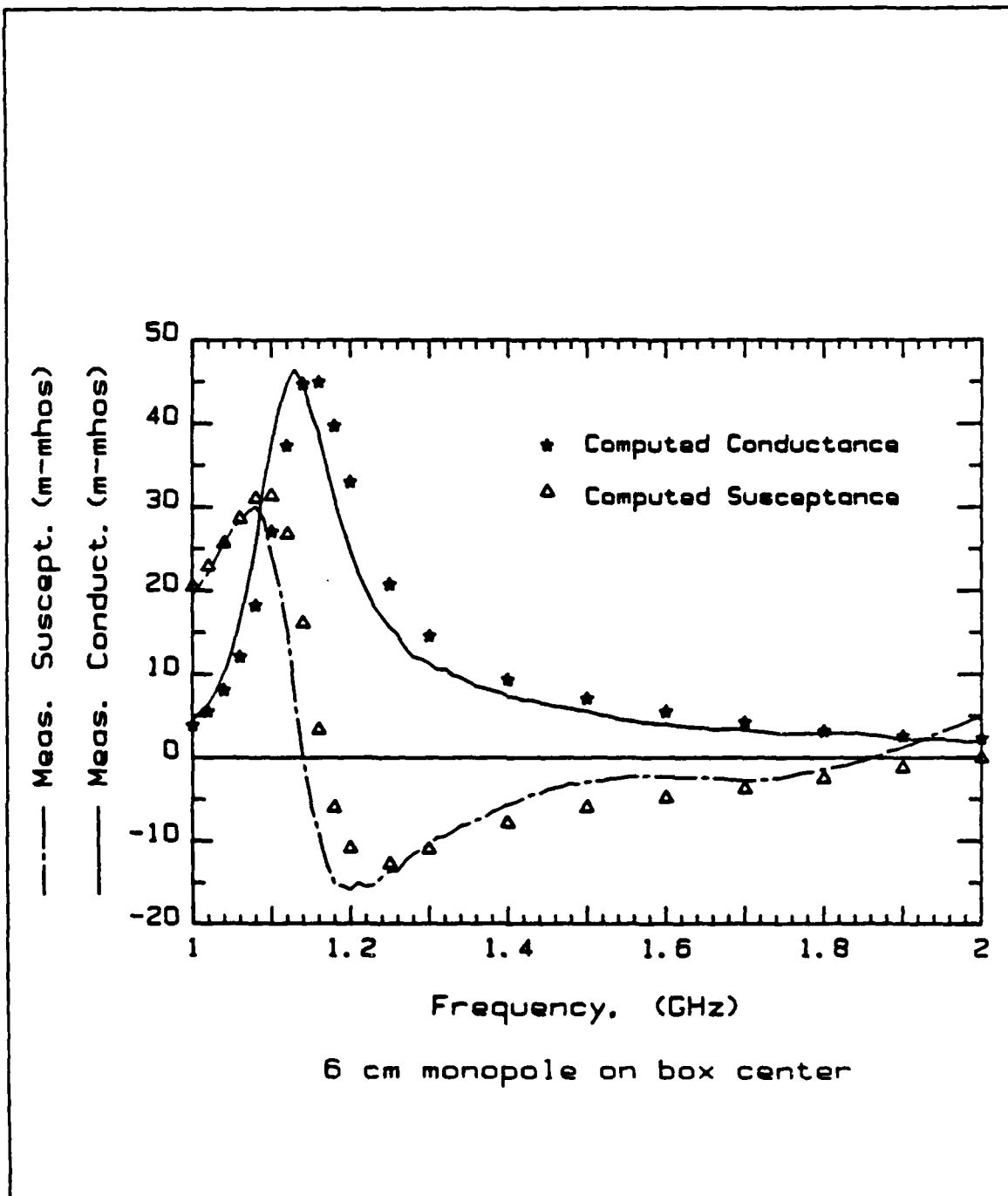
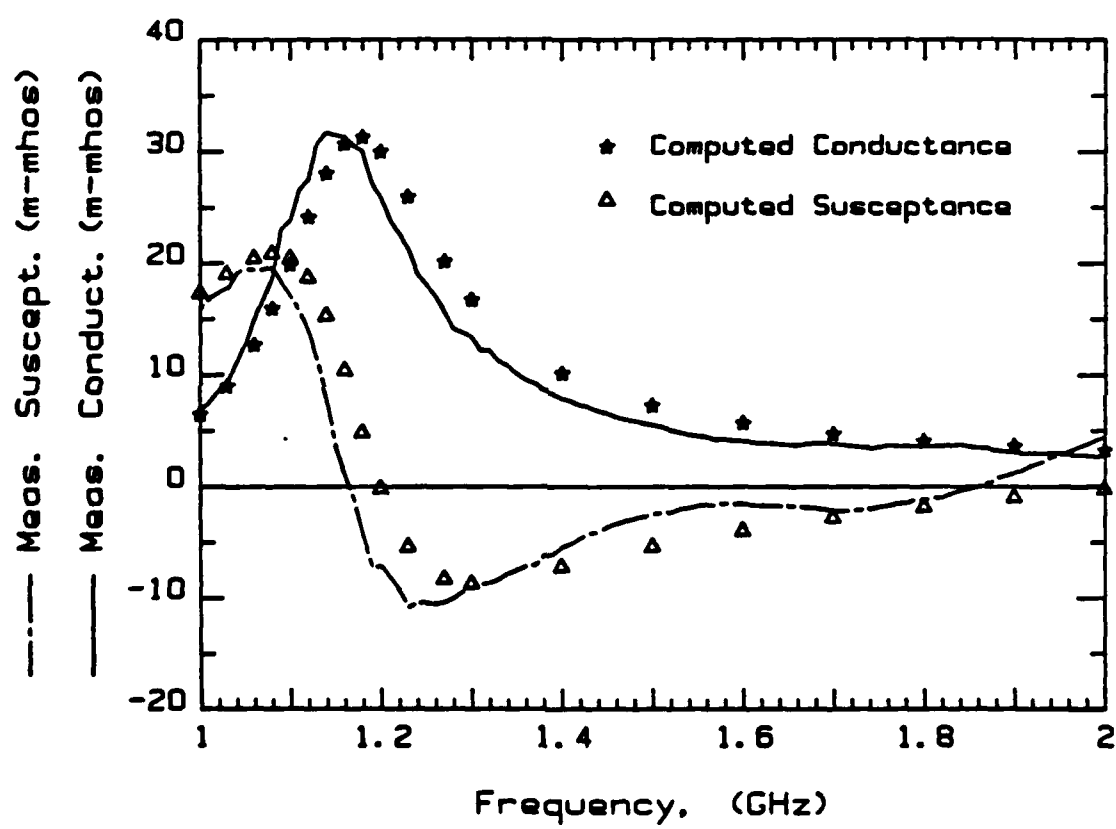
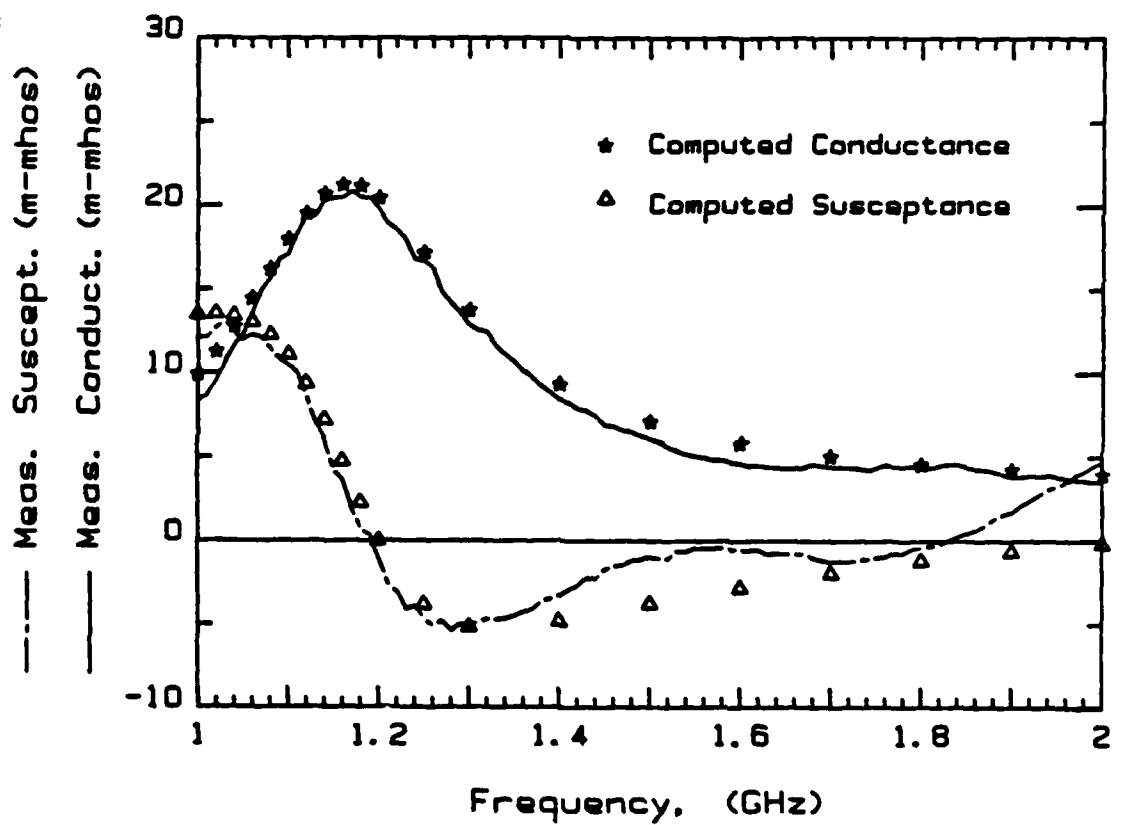


Figure D.4: 6 cm Monopole at box center



6 cm monopole on box edge(center-4)

Figure D.5: 6 cm Monopole at box edge(center-4)



6 cm monopole on box corner(diag. center-5)

Figure D.6: 6 cm Monopole at box corner(diagonal center-5)

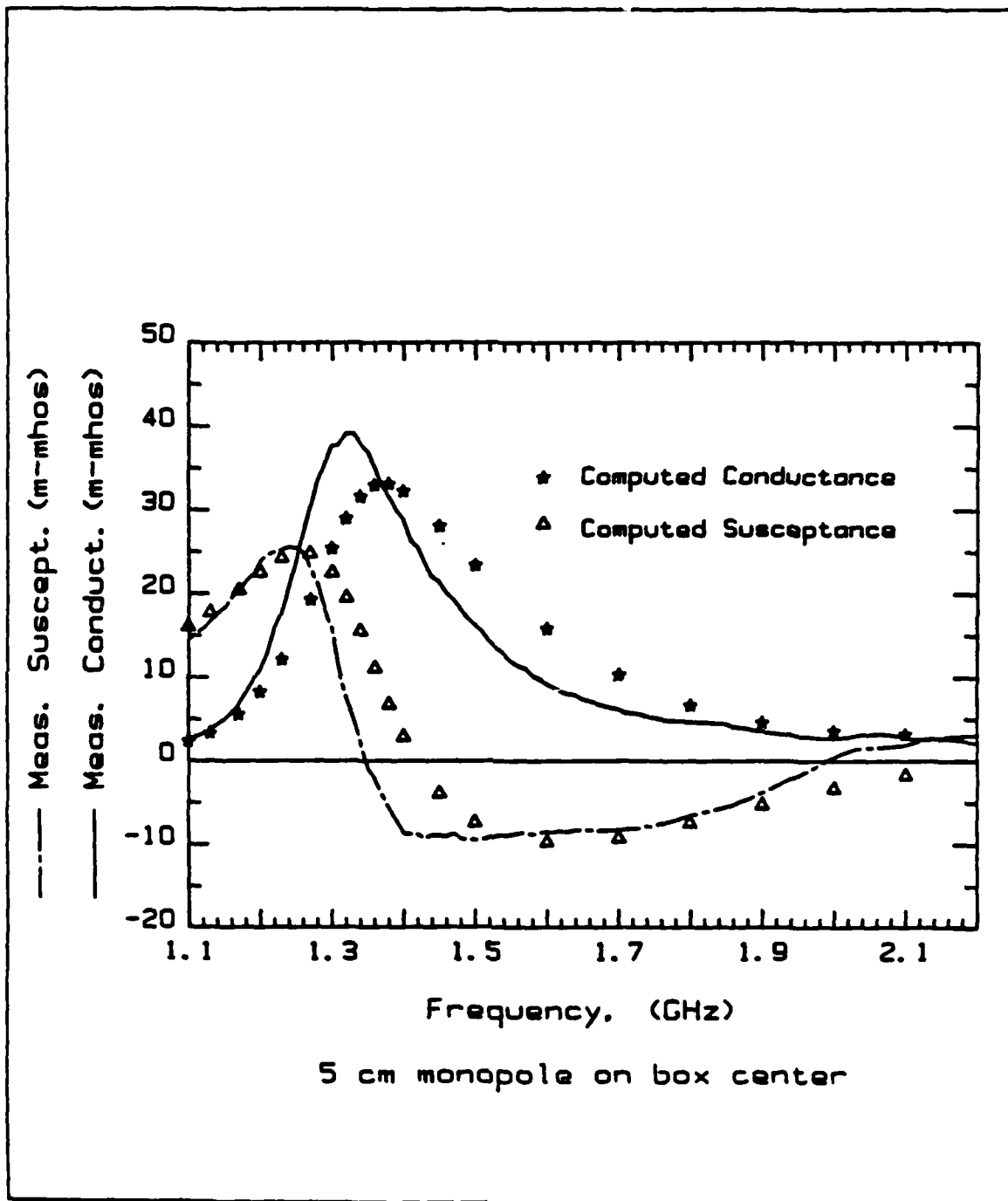


Figure D.7: 5 cm Monopole at box center



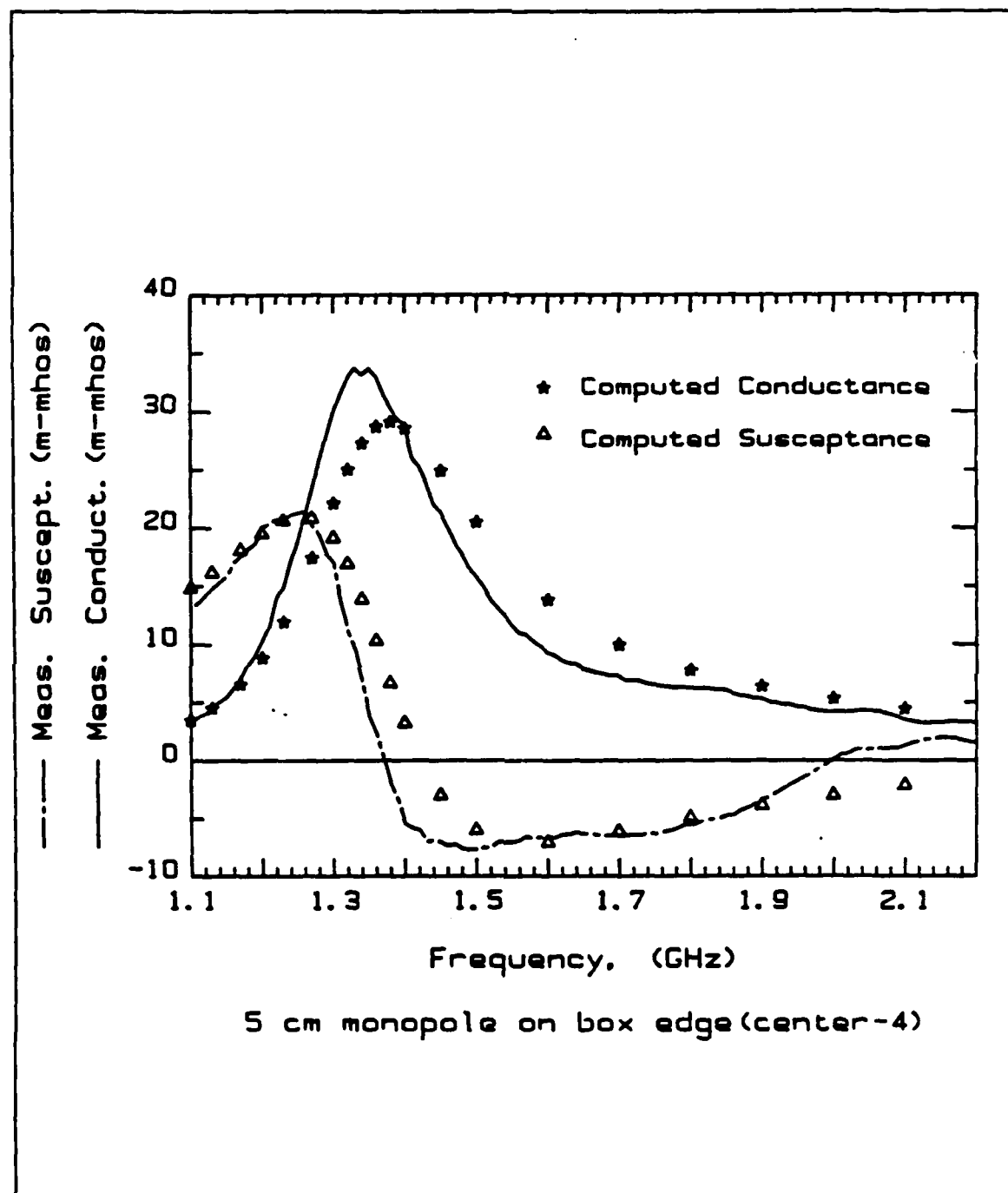


Figure D.8: 5 cm Monopole at box edge(center-4)

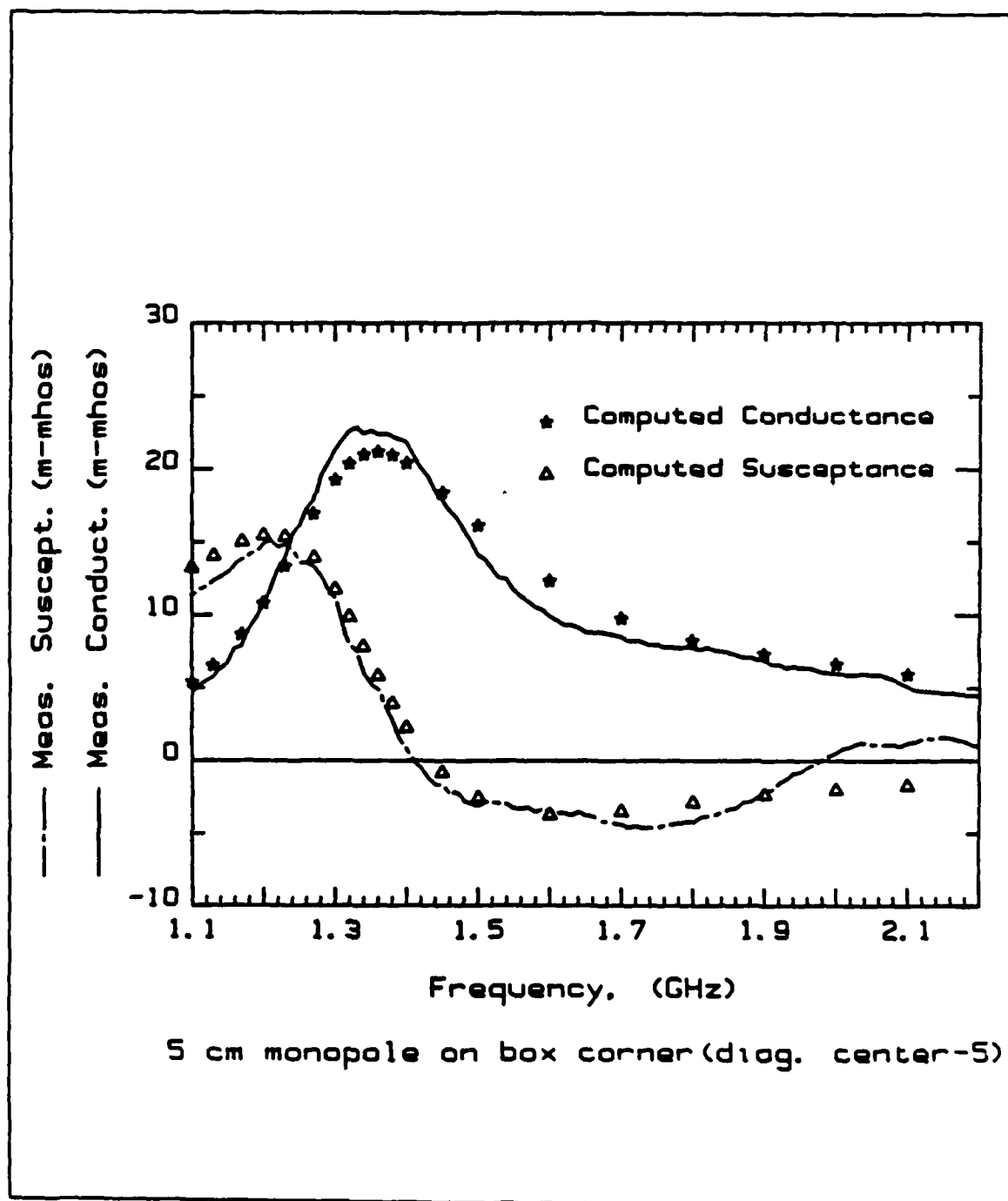


Figure D.9: 5 cm Monopole at box corner(diagonal center-5)

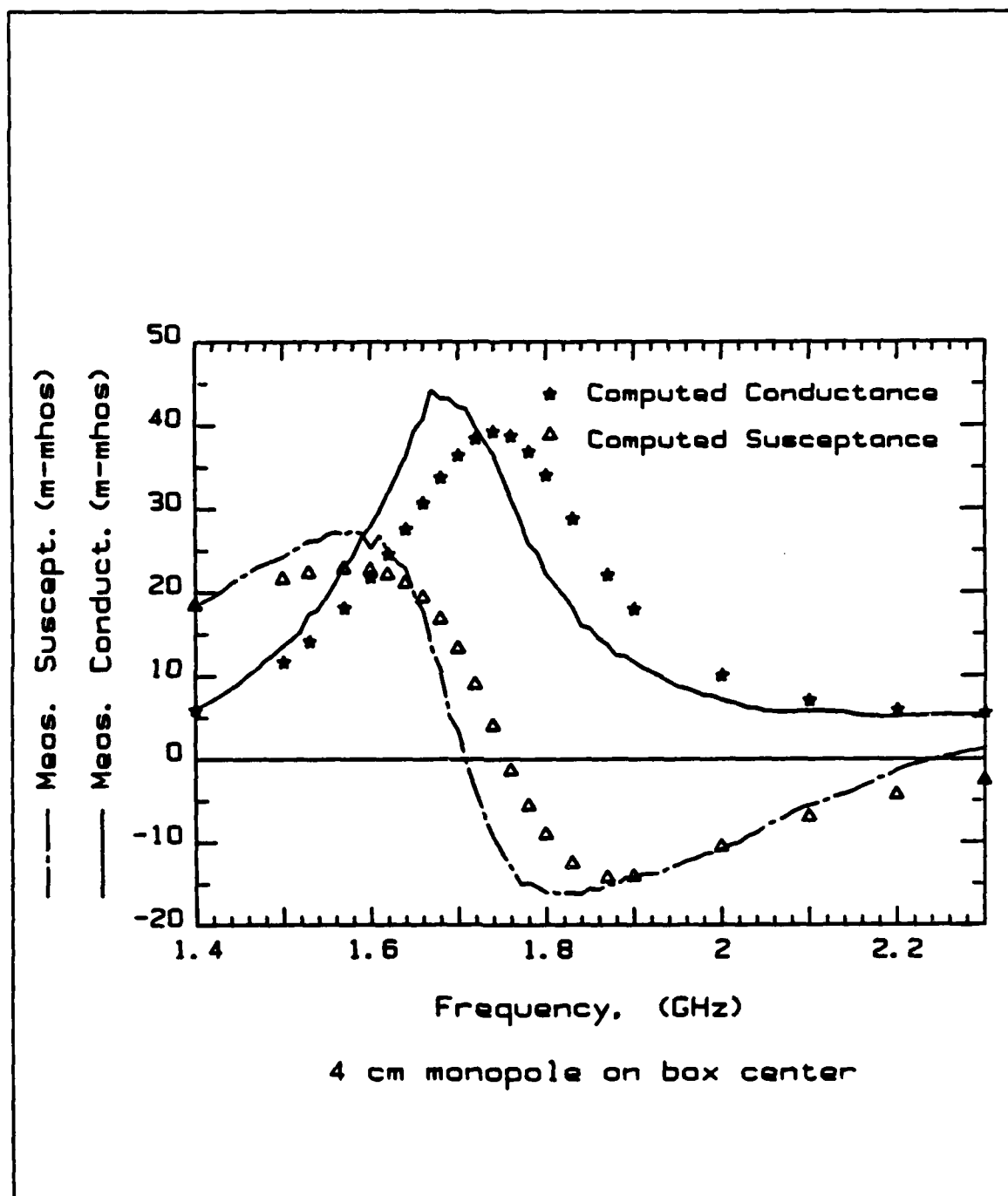


Figure D.10: 4 cm Monopole at box center

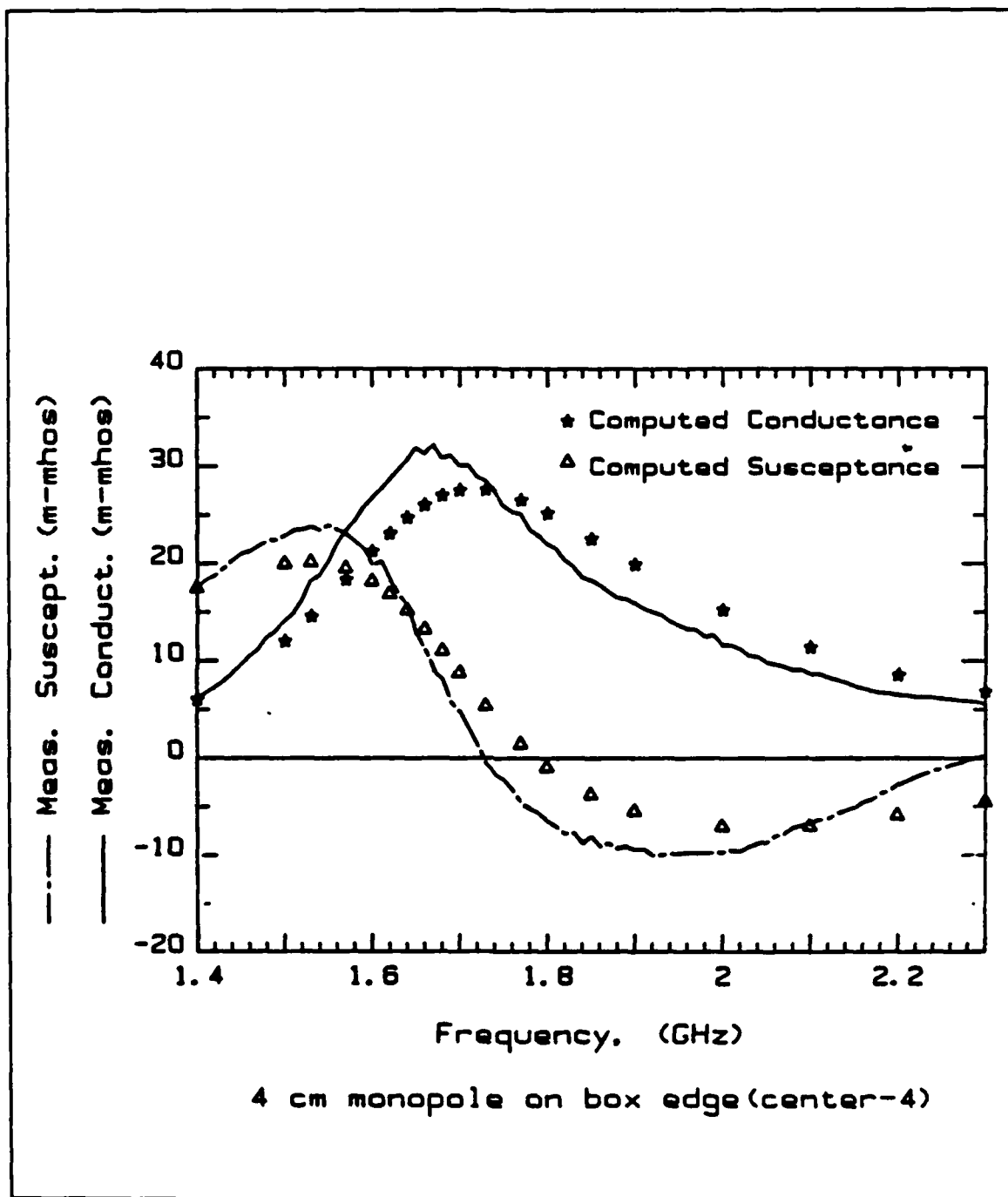
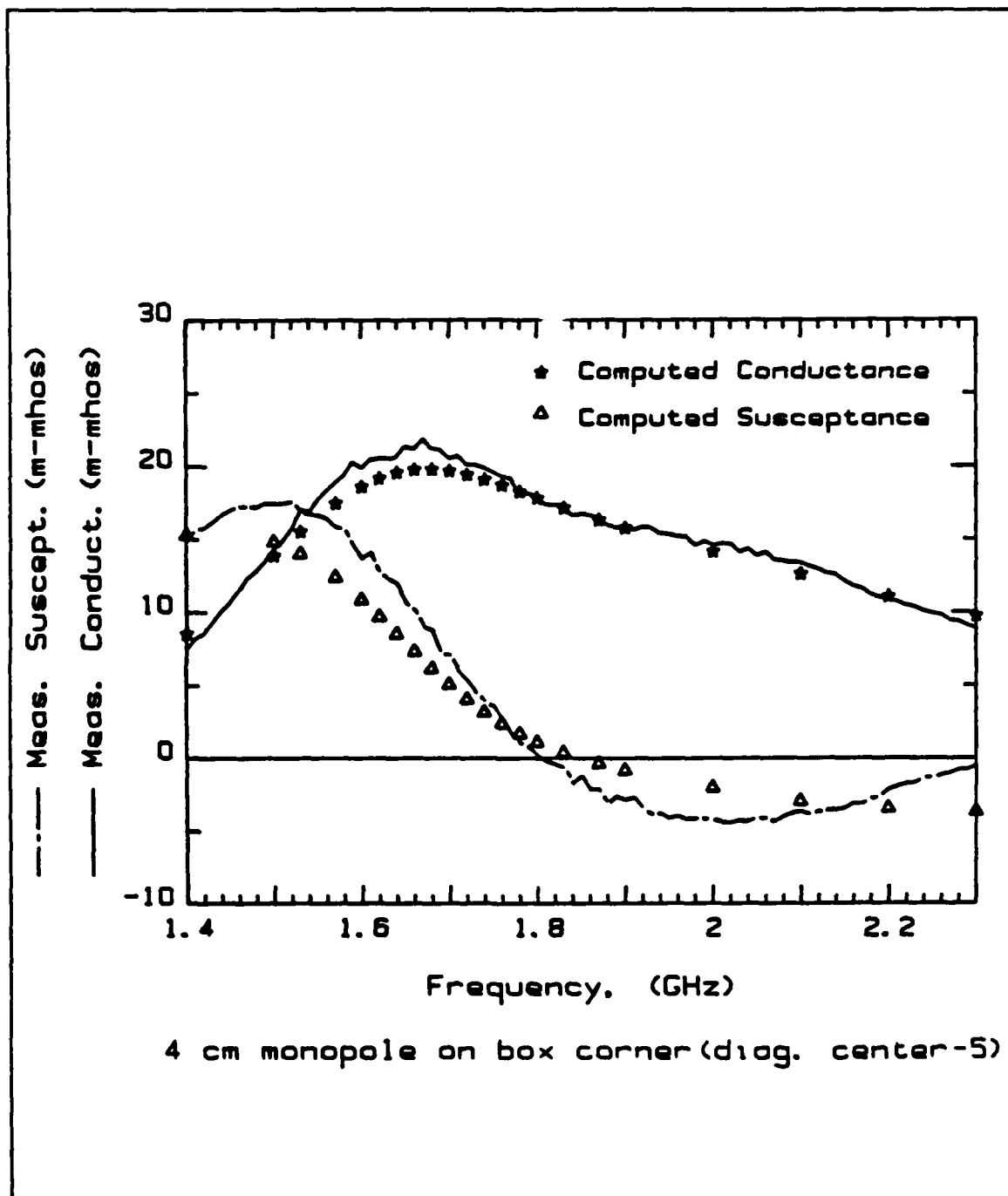


Figure D.11: 4 cm Monopole at box edge(center-4)



4 cm monopole on box corner(diag. center-5)

Figure D.12: 4 cm Monopole at box corner(diagonal center-5)

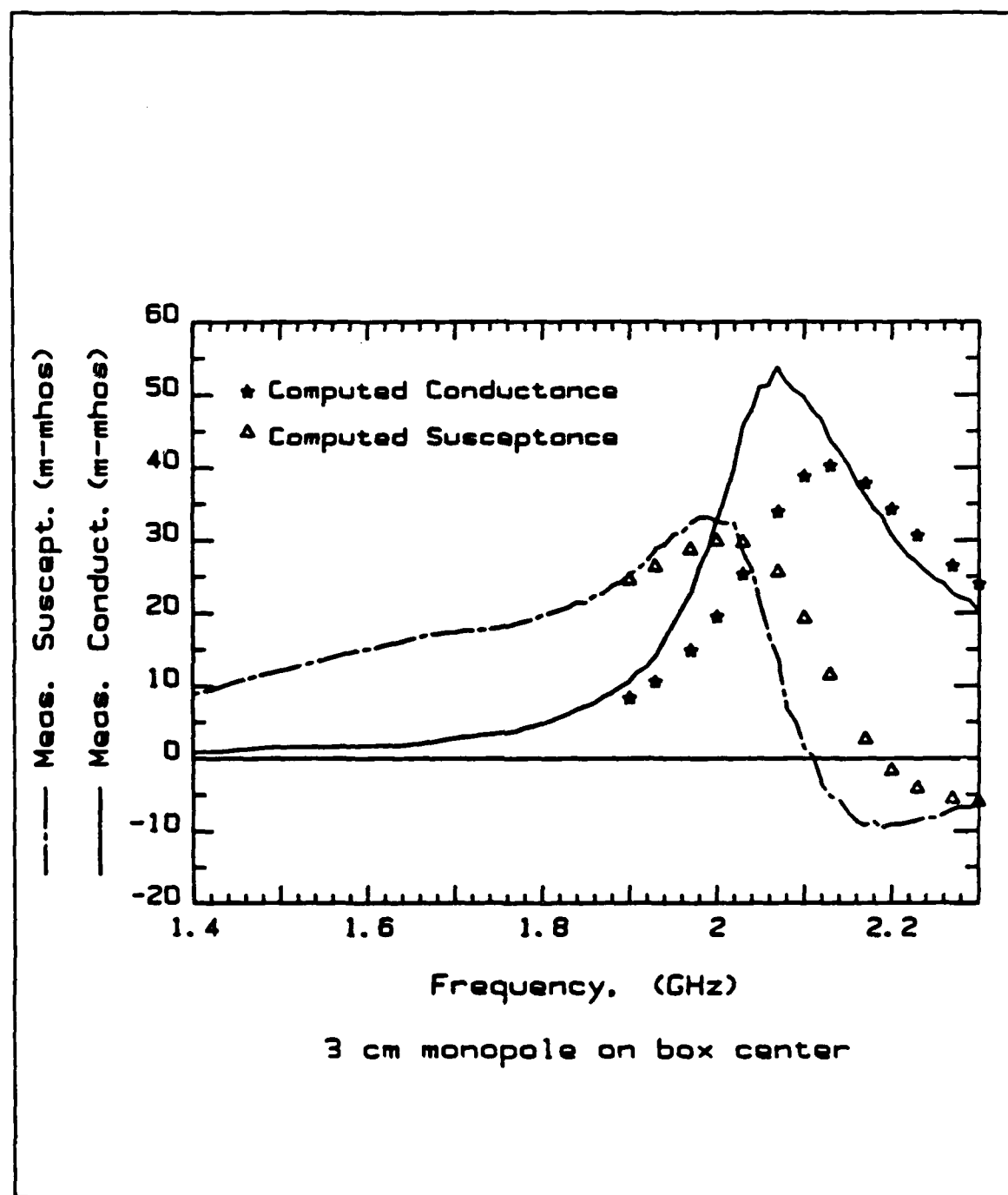


Figure D.13: 3 cm Monopole at box center

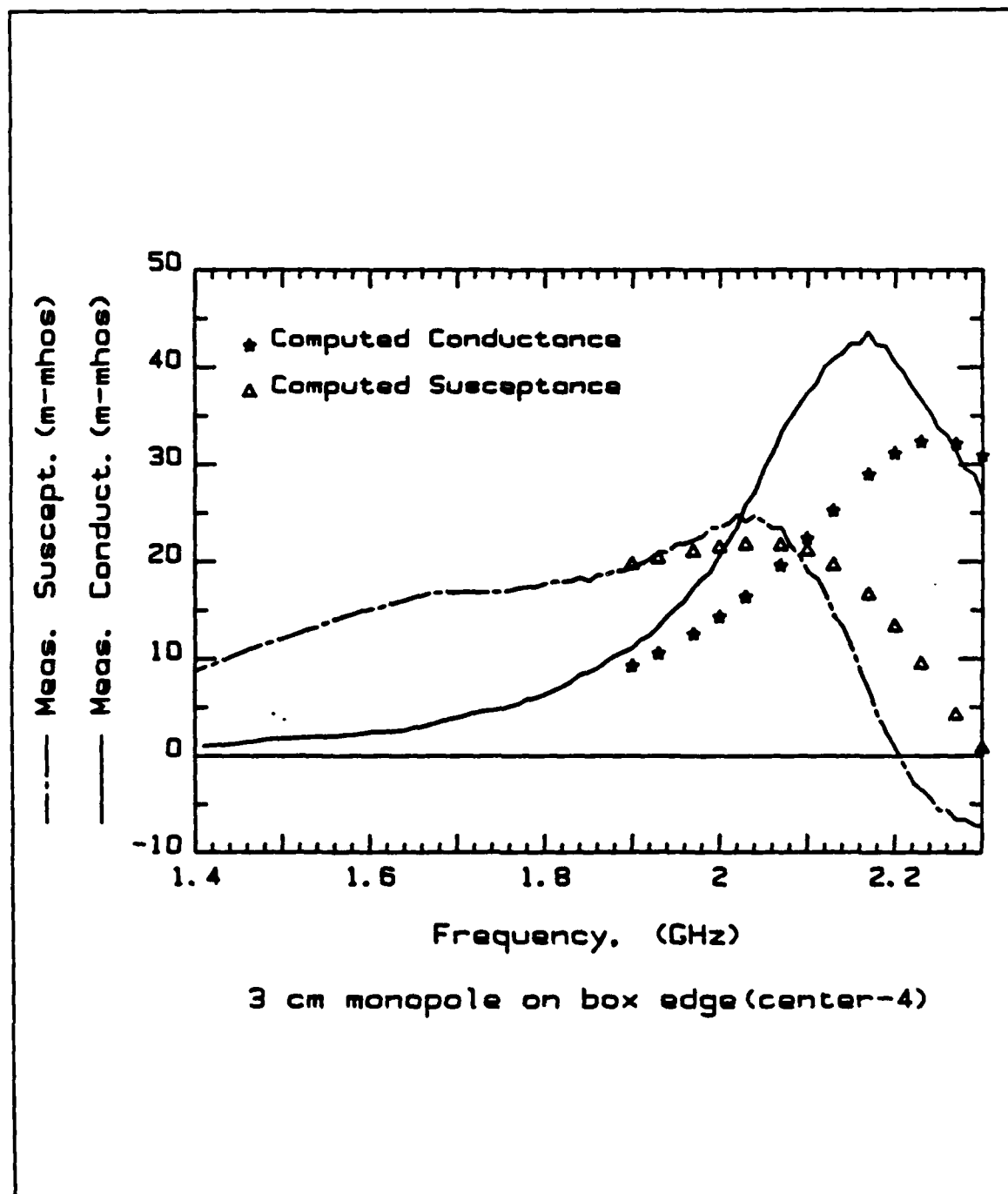


Figure D.14: 3 cm Monopole at box edge(center-4)

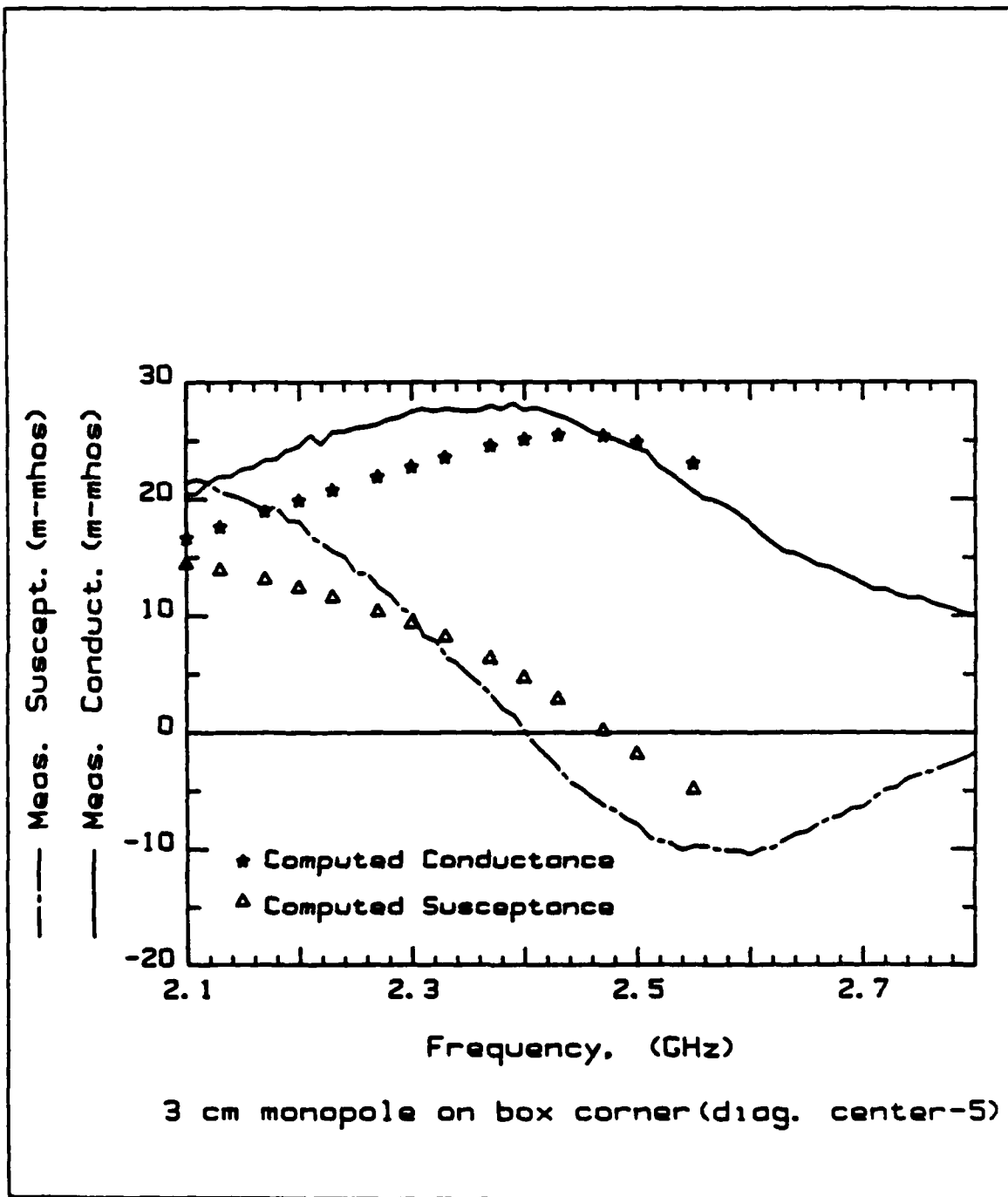


Figure D.15: 3 cm Monopole at box corner(diagonal center-5)



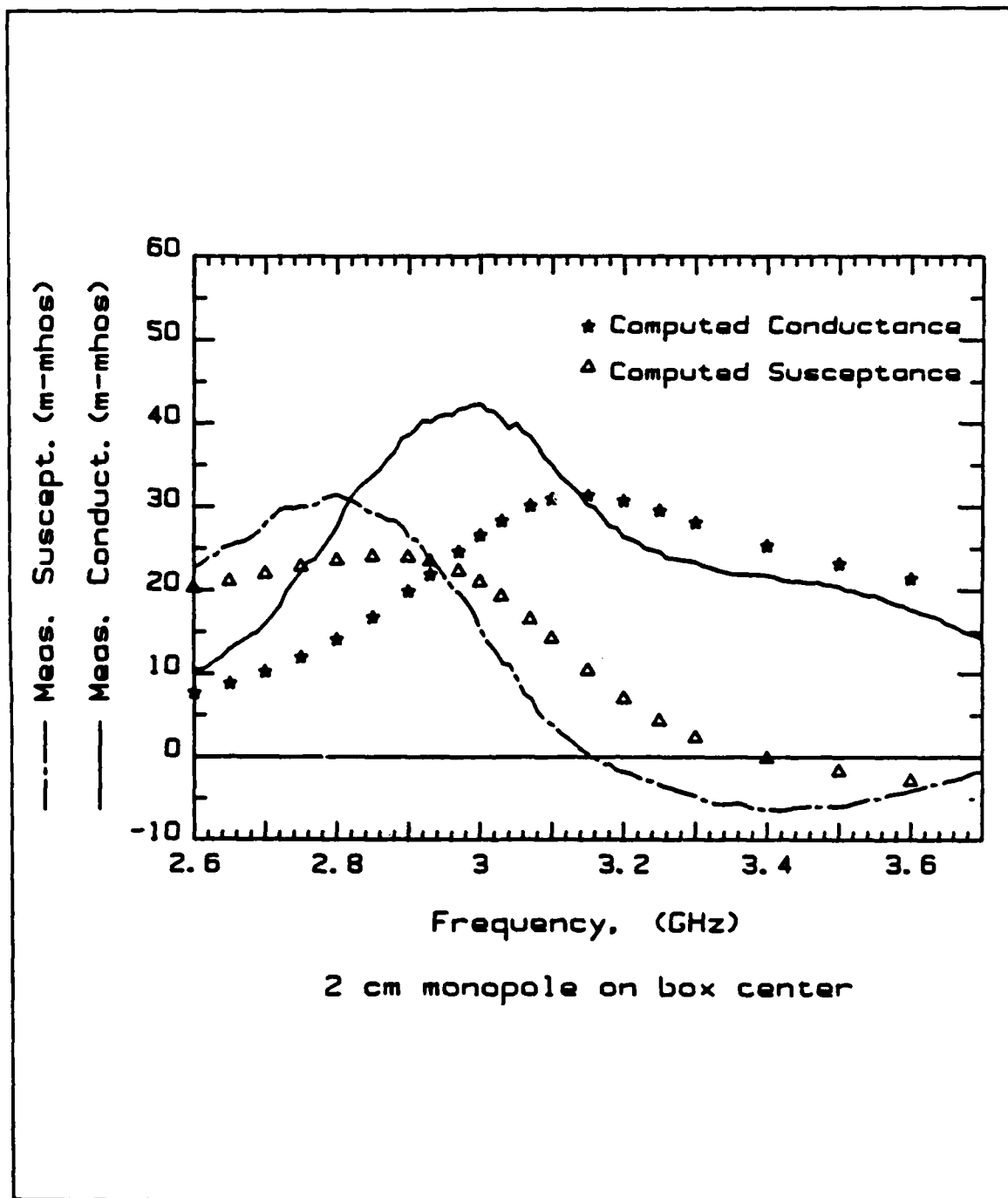


Figure D.16: 2 cm Monopole at box center

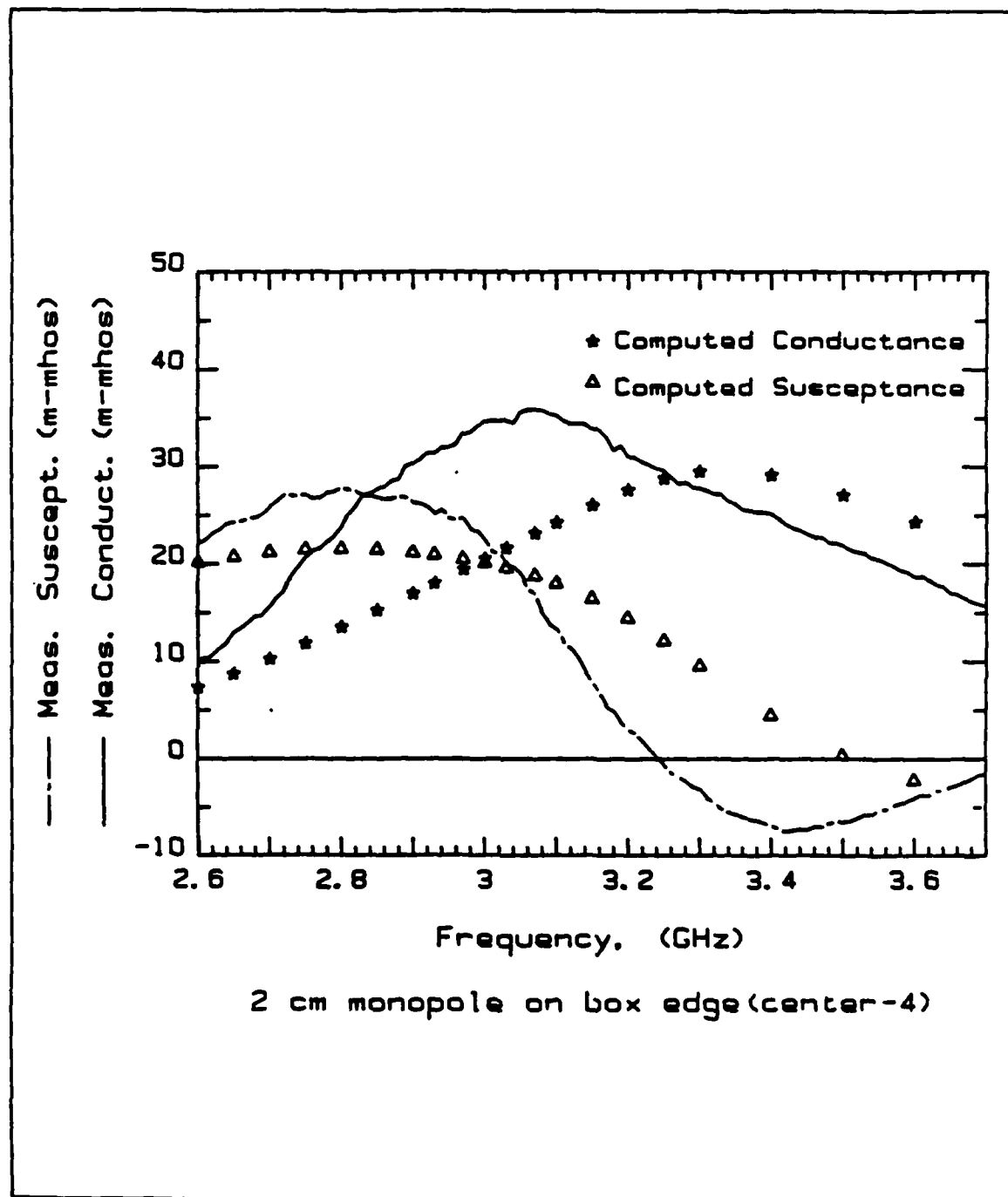


Figure D.17: 2 cm Monopole at box edge(center-4)

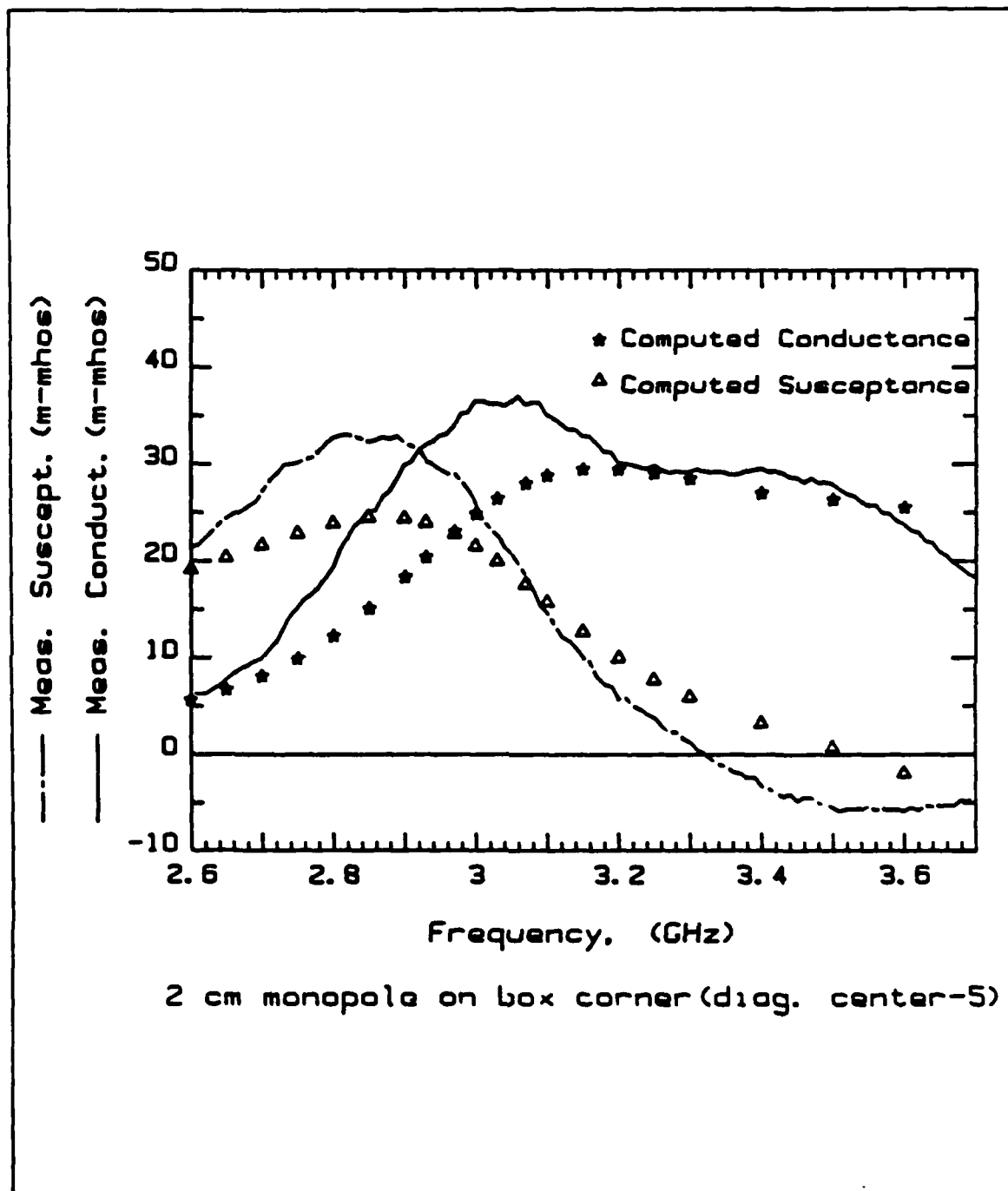


Figure D.18: 2 cm Monopole at box corner(diagonal center-5)

## Appendix E

### Conclusion

After the collection of the admittance measurements for monopoles on a conducting box over a ground plane is completed, the significance of all these data should be addressed. The purpose of all this data collection was to see how the circuit parameters such as peak input conductance, zero crossing frequency of the input susceptance and quality factor are affected as the position of the monopole changes with respect to the center of the box.

From the superimposed admittance versus frequency plots shown in Figures C.1 through C.10 it is clearly seen that the peak input conductance is a maximum when the monopole is at the box center and it decreases as the monopole position shifts away from the center of the box either toward the edge of the box or the corner of the box. This trend is observed for all lengths of monopoles considered except for the 2 cm monopole where peak input conductance is not maximum when the monopole is at the center of the box. Figures C.16 through C.20 also depict how the peak input conductance varies with the position of the monopole with respect to the center of the box.

The general observation that can be made about the zero crossing frequency of the input susceptance is that it always increases as the monopole position moves

away from the center. This is observed in Figures C.1 through C.10 and can be clearly noticed in Figures C.21 through C.25. This zero crossing frequency of the input susceptance is minimum when the monopole is at the box center and gradually increases to its maximum when the monopole is at the corner of the box. Again there is a small deviation in this trend for the 2 cm monopole which may be due to experimental error.

Figures C.11 through C.15 show how the quality factor is affected by the position of the monopole with respect to the center of the box. The quality factor, like the peak input conductance, decreases as the monopole position shifts away from the center. The quality factor is a maximum when the monopole is at the center, and monotonically decreases as the distance of the monopole from the center increases.

In chapter 4, we have discussed computation of input admittance for a monopole on a box over a ground plane. Figures D.7 through D.21 show comparisons of measured data to numerically computed ones. The agreement in general is very good for the 6 cm and 5 cm monopoles. For the 4 cm and smaller lengths of monopoles the agreement deteriorates. It is likely that one probably needs to use smaller triangular patches in modelling the box to improve the accuracy for the smaller monopole lengths.

# Bibliography

- [1] M. Marin and M. F. Catedra, '*Input Impedance of an Off-Axis Monopole on a Circular Disk*', IEEE Antenna and Propagation Society Intl. Symposium Digest, pp APS-8-3, 1985.
- [2] D. M. Pozar and E. H. Newman, '*Analysis of a Monopole Mounted Near an Edge or a Vertex*', IEEE Trans. Antenna and Propagation, Vol. 30, May 1982.
- [3] K. H. Awadalla and T. S. M. Maclean, '*Input Impedance of a Monopole Antenna at the Center of a Finite Ground Plane*', IEEE Trans. Antennas and Propagation, Vol. AP-26, No. 2, March 1978.
- [4] S. M. Rao, D. R. Wilton and A. W. Glisson, '*Electromagnetic Scattering by Surfaces of Arbitrary Shape*', IEEE Trans. Antennas and Propagation, Vol. AP-30, No. 3, May 1982.
- [5] Ronald W. P. King, '*The Theory of Linear Antennas*', Harvard University Press, Massachusetts, 1956.

END

DTIC

7-86